R.F. Note #120
August 23, 1999

Tim Berenc
John Brandon, John Vincent

The Dee-Voltage Regulator Module Upgrade

Introduction

This RF note presents the upgrade design of the dee-voltage regulation module. Its intent is to provide a thorough discussion of the dee-voltage regulation system, including the K500 and K1200 cyclotron resonators. The focus is placed upon the closed-loop system design with particular attention to the stability and noise-rejection performance of the entire voltage-regulation system.

A block-diagram of the voltage-regulation system is shown below:

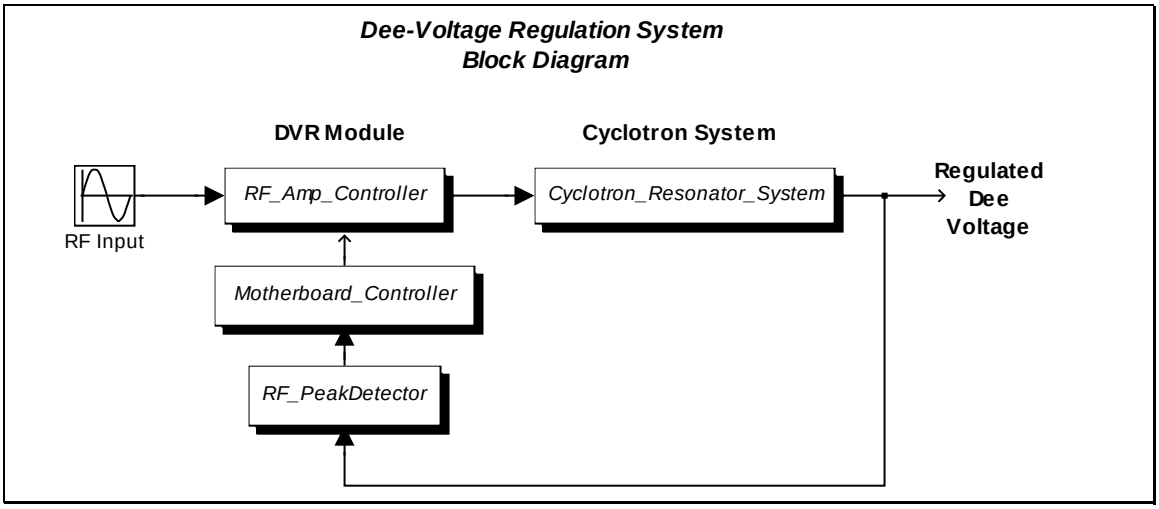

The Dee-Voltage Regulation (DVR) module consists of the actuator (the RF Amplitude-Controller), the controller (the Motherboard), and the feedback sensor (the RF Peak-Detector). The cyclotron system consists of the RF transmitters and the RF resonating structures.

All the components of the system are discussed in this note. However, the discussion is begun with a characterization of the cyclotron system since this is the system for which the DVR was designed.

Cyclotron Resonator Dynamic Response Characterization

The 'Cyclotron Resonator System' consists of a RF transmitter and a dee-resonator and all the low-level electronics which interconnect with the RF transmitter (outside those modules directly used for amplitude regulation). However, the component within this system which dominates the dee-subsystem's response to voltage amplitude-modulations is the dee-resonator itself. As noted in RF Note 118, it is the fairly high quality factor, Q, (roughly 3000-6000) of a dee-resonator which limits its frequency response to amplitude-modulations. As for the RF transmitter, it has little influence on the dee-subsystem's response since its tank circuits have very low Q values of around 10. And if the low-level electronics are viewed as having a Q-factor, they too would have little influence on the dee-subsystem's response since they are designed to operate over a large RF bandwidth; thus effectively resulting in very low Q-factors. To understand how the Q-factor affects a resonator's response to amplitude-modulations, please see Appendix A. As a matter of fact, this appendix is a revision to the appendix offered in RF Note 118.

Previously, RF Note 118 had provided a simple single-pole low-pass filter (LPF) model for a dee-resonator's response to amplitude-modulations. However, a more detailed analysis of the amplitude-modulation process within a general electromagnetic resonator gives a different model. The detailed account of this analysis is included in Appendix A for the interested reader. For those who just want the general gist of the analysis given in the appendix, the following generalizes the results:

> Using a parallel RLC equivalent circuit model for an electromagnetic resonator, the amplitude modulation response was determined mathematically, using Fourier transforms, to be a LPF-like function, but it does not consist of a single pole. Instead, it consists of one real zero and two complex conjugate poles. In the limit as Q approaches infinity, the two complex conjugate poles close in on the real zero, thereby resulting in a single-pole LPF after a pole/zero cancellation. However, this single-pole also approaches zero in the limit as Q approaches infinity and thus, the resonator becomes practically incapable of supporting any sort of amplitude modulations. As the Q-factor is lowered, the zero/complex-conjugate-pole pair moves increasingly to the left in the s-plane while simultaneously becoming more separated.

This mathematical formulation is very important to the analysis of the amplitude-regulation loop since it is the dee-resonator which dominates the response not only of the dee-subsystem but of the entire amplitude-regulation loop as will be seen once the dynamic responses of the dee-voltage regulator components are characterized.

Now, the dee-resonator's Q-factor is a function of the RF operating frequency. In particular, the Q-factor goes down as the RF operating frequency is increased. Thus, the dee-resonator's response to amplitude-modulations will also change with the operating frequency. Mathematically, the resonator's zero/complex-conjugate-pole pair moves increasingly to the left in the s-plane as the RF operating frequency increases. This is represented in figure 7 for the K1200. The K1200 data was calculated using the RLC resonator parameters derived from actual power-loss measurements made in [1].

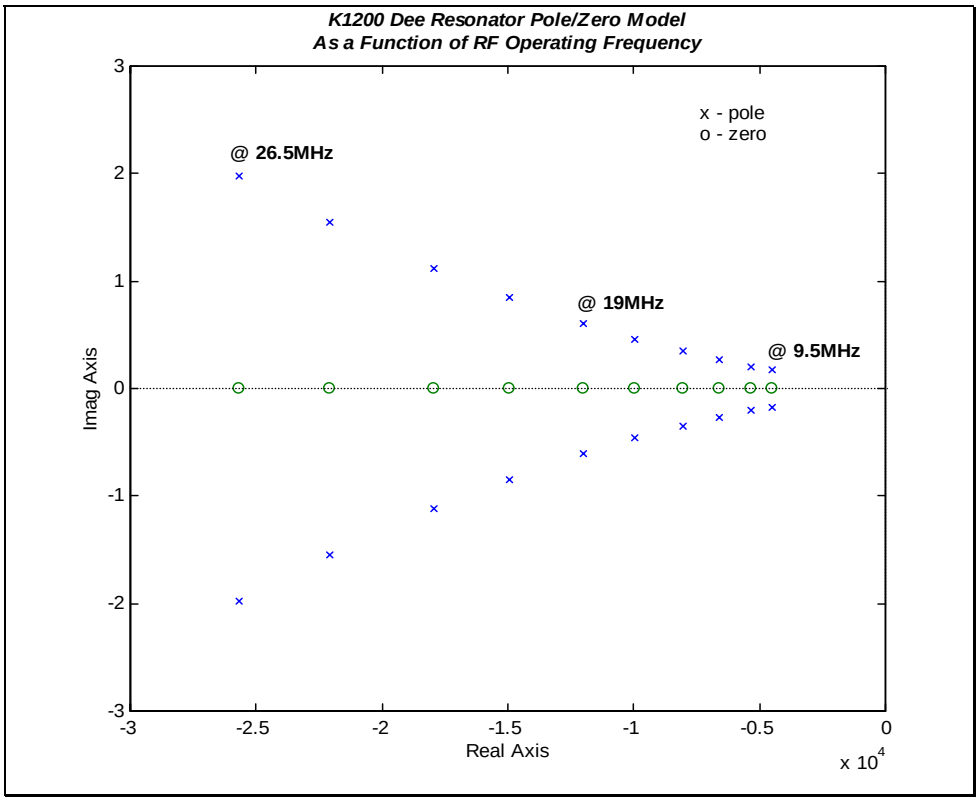

Figure 7: K1200 Dee Resonator Pole/Zero Locations as a Function of RF Frequency

The describing transfer function is expressed as,

$$Cyc(s) = \frac{p \cdot p^*}{z} \cdot \frac{(s+z)}{(s+p)(s+p^*)} \qquad (1)$$

where z is the zero location, and p and p^* are the complex conjugate pole locations. The scaling factor normalizes the gain to be unity at DC.

A list of the K1200 zero and pole locations across the operating frequency range are given in the following table.

K1200 Dee Resonator Transfer Function zero and poles

Freq. (MHz)	zero (z) $x10^3$	pole (p)
9.5	4.486	4486 + i 0.1686
11	5.363	5363 + i 0.2081
13	6.603	6603 + i 0.2669
15	8.062	8062 + i 0.3448
17	9.957	9957 + i 0.4640
19	12.008	12008 + i 0.6039
21	14.967	14967 + i 0.8488
23	17.930	17930 + i 1.112
25	22.074	22074 + i 1.551
26.5	25.687	25687 + i 1.981

The above zero and pole locations were calculated using the formula derived in Appendix A. The parallel RLC resonator parameters for the K1200 are listed in the following table:

K1200 Dee Resonator Equivalent RLC parameters

Freq. (MHz)	Q	R_{shunt} (kΩ)	C_{shunt} (pF)	L_{shunt} (nH)
9.5	6653	196.43	567.4	494.7
11	6444	175.13	532.4	393.2
13	6185	153.09	494.6	303.0
15	5845	134.19	462.2	243.6
17	5364	115.92	433.2	202.3
19	4971	102.47	406.4	172.7
21	4408	86.95	384.2	149.5
23	4030	77.87	358.1	133.7
25	3558	67.19	337.1	120.2
26.5	3241	59.69	326.1	110.6

As for the K500, its pole/zero locations as a function of RF operating frequency are depicted in figure 8. This CCP K500 data was determined from theoretical analyses performed in RF Note 116, 'CCP K500 Tuning Stem Design'.

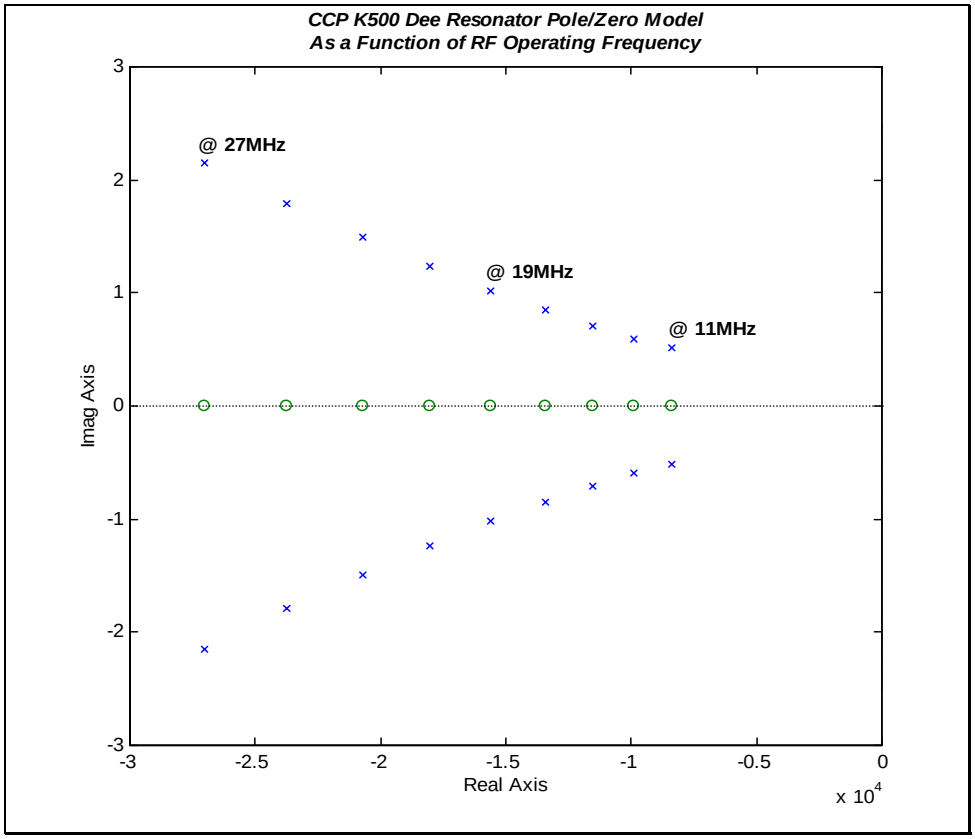

Figure 8: CCP K500 Dee Resonator Pole/Zero Model as a Function of RF Frequency

A list of the K500 zero and pole locations for the transfer function given in equation (1) are listed in the following table:

K500 Dee Resonator Transfer Function zero and poles

Freq. (MHz)	zero (z) $x10^3$	pole (p)
11	8.402	8402 + i 0.5107
13	9.877	9877 + i 0.5971
15	11.547	11547 + i 0.7074
17	13.446	13446 + i 0.8463
19	15.593	15593 + i 1.018
21	18.021	18021 + i 1.231
23	20.734	20734 + i 1.487
25	23.750	23750 + i 1.795
27	27.048	27048 + i 2.156

The above zero and pole locations were calculated using the formula derived in Appendix A. The parallel RLC resonator parameters for the K500 (from simulations performed in RF Note 116) are listed in the following table:

K500 Dee Resonator Equivalent RLC parameters

Freq. (MHz)	Q	R_{shunt} (kΩ)	C_{shunt} (pF)	L_{shunt} (nH)
11	4113	98.81	602.3	347.6
13	4135	89.35	566.6	264.4
15	4081	80.68	536.7	209.7
17	3972	72.94	509.8	171.9
19	3828	66.17	484.6	144.7
21	3661	60.25	460.5	124.7
23	3485	55.12	437.5	109.4
25	3307	50.68	415.4	97.52
27	3136	46.83	394.8	87.95

As was mentioned earlier, due to the low Q-factor of the RF transmitter's tank circuits, their zero/complex-conjugate-pole pair is so far to the left in the s-plane that they can be neglected. In particular, the Q-factors were found theoretically to be around 10. This corresponds to a zero/complex-conjugate-pole pair location at around 350-400kHz.. For all practical purposes, the RF transmitter model can be neglected within the 'Cyclotron Dee Subsystem'. Thus, the mathematical description of the 'Cyclotron Dee Subsystem' component of figure 6 consists solely of the dee-resonator's transfer function.

The Transmitter/Resonator Open-Loop Gain

The open-loop gain of the resonator system is defined as the voltage gain from the output of the DVR to the voltage on the dee-resonator. This gain is influenced by the 50-Watt amplifier, the RF transmitter, and the dee-resonator. Below is a block diagram representing this open-loop gain chain.

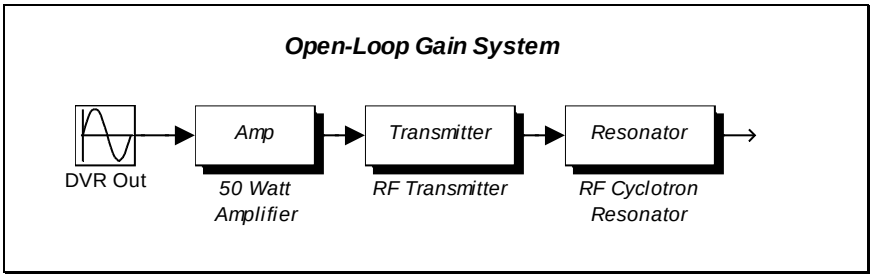

The 50-Watt amplifier is a fixed gain that does not depend upon operating level or frequency. However, the RF transmitter gain and the RF resonator gain are dependent upon both the operating RF voltage level and the operating RF frequency.

The 50-Watt Amplifier Open-Loop Gain

The 50-Watt amplifier is a fixed gain. However, currently there are two types of 50Watt amplifiers; those on the K1200 and those on the K500. The actual gain of these amplifiers is tabulated in the following table.

50-Watt Amplifier Gain

	Gain (dB)	Voltage Gain (V/V)
K500	44	158.5
K1200	47	223.9

The Transmitter Open-Loop Gain

The RF transmitter gain is predominantly a function of the operating RF voltage as opposed to RF frequency. The dependency on operating RF voltage is a result of the inherent non-linearities of the tubes within the transmitter. The tubes exhibit very little dependency on RF operating frequency.

The gain of the TH555 tube as a function of RF anode voltage was investigated using a software program developed by John Vincent called *WinTube*. For a fixed load impedance of 1340.9 Ω presented to the anode, the voltage gain from grid to the anode was determined by simulating the tube operation at various grid voltage drive levels. The data is plotted as a function of anode voltage since the dee-voltage is directly proportional to the tube anode voltage as will be seen in further discussions. Furthermore, since the operating dee-voltage is the ultimate goal, it is pertinent to know the variation of the system gain as a function of operating voltage. The results are displayed in the following figure. The data used for the graph can be found in the table proceeding the figure.

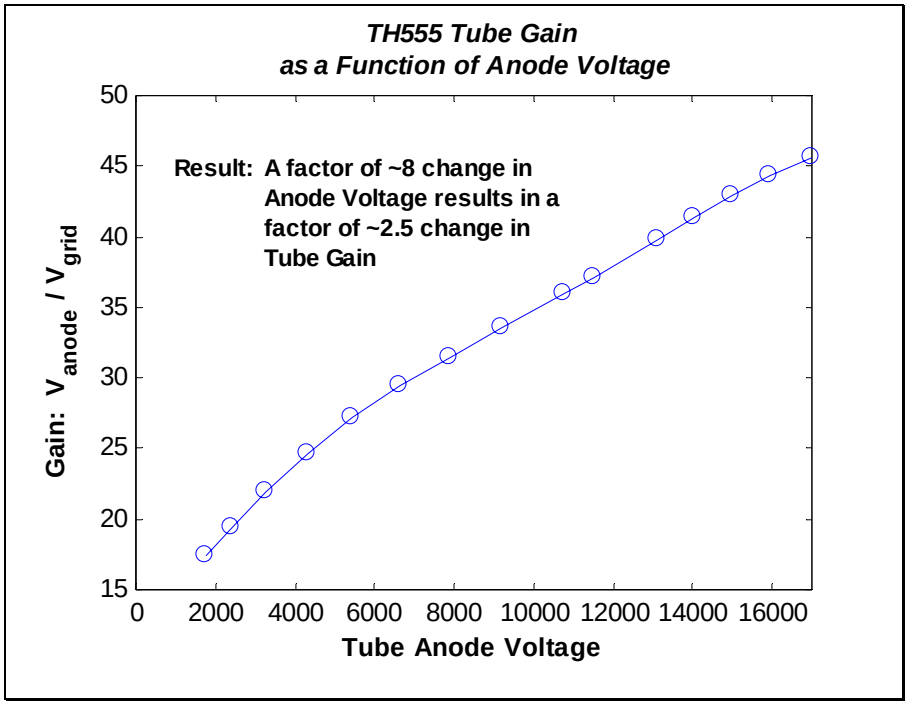

Simulated TH555 Voltage Gain Data at 27MHz

Grid Volts (Vpk)	Anode Volts (Vpk)	Gain (Anode/Grid)
100	1743	17.4
125	2429	19.4
150	3284	21.9
175	4304	24.6
200	5443	27.2
225	6641	29.5
250	7877	31.5
275	9214	33.5
300	10782	35.9
310	11509	37.1
330	13152	39.9
340	14057	41.3
350	14998	42.9
360	15953	44.3
373	17000	45.6

From the graph, it is noted that a change in anode voltage by a factor of approximately 8 results in a change in the tube gain by a factor of approximately 2.5. Since the anode voltage is directly proportional to the dee-voltage, the same change in dee-voltage will result in the same change in gain.

The Resonator Open-Loop Gain

The RF resonator gain, on the other hand, is predominantly a function of the operating RF frequency as opposed to the RF voltage level. The dependency on RF frequency is due to the change in shunt-impedance across the operating frequency range. In particular, the shunt-impedance goes down as the frequency increases. Thus, it takes more power at higher frequencies than at lower frequencies for the same dee-voltage. This increase in required power implies that the voltage gain of the resonator decreases as a function of frequency.

Assuming that the transmitter's output coupling capacitor is set to present the same load impedance to the tube across the operating frequency range, it becomes clear how this frequency-dependent gain arises. For a certain DVR RF output voltage, V_{DVR}, a linearly related anode voltage swing, $V_A = k \cdot V_{DVR}$ will result. The linear relationship between V_{DVR} and V_A results from the following:

> V_A is linearly related to the anode current, I_A, through R_A, the load impedance presented to the anode of the tube. Furthermore, I_A is linearly related to the tube's grid voltage which in-turn is directly related to the voltage from the 50-Watt amplifier. Finally, the voltage from the 50-Watt amplifier is directly related to the DVR RF output voltage V_{DVR}.

With this $V_A = k \cdot V_{DVR}$ the tube will be providing $P = \frac{(V_A)^2}{R_A}$ Watts of power. If the output coupling capacitor forces R_A to be the same at all frequencies, then for the same V_A (or V_{DVR}) at two different frequencies, the transmitter will be providing the same amount of power, P. The dee-voltage resulting from this amount of power is determined from the resonator shunt-impedance, $R_S(f)$, as $V_{Dee}(f) = \sqrt{P \cdot R_S(f)}$. Since $R_S(f)$ decreases as a function of frequency, the dee-voltage obtained also decreases as a function of frequency. The gain of the resonator is thus given as:

$$K_{Res}(f) = \frac{V_{Dee}}{V_A} = \sqrt{\frac{R_S(f)}{R_A}}$$

The exact value of K_{Res} is not critical; rather, the variation in gain as a function of frequency is of concern. Thus, the resonator gain is normalized with respect to the gain at the highest operating frequency for each cyclotron. The highest operating frequency is chosen due to the lowest value shunt-impedance occurring there. From the above discussion, the open-loop gain of the resonators goes down as a function of frequency. Thus, the full-scale DVR RF output voltage feeding the 50W amplifier has to be at least that amount of RF output voltage needed to obtain the full-scale dee-voltage at the highest frequency. In particular, a 0-10Volt command signal to the DVR will correspond to 0-Full-Scale Dee Voltage only at the highest frequency. At lower frequencies, 10Volts will correspond to some Dee-voltage higher than full-scale; implying an increase in open-loop gain.

For a given power level, P, provided by the transmitter, the resultant dee-voltage at the highest operating frequency, f_H, is given as $V_{Dee}(f_H) = \sqrt{P \cdot R_S(f_H)}$. For the same P at frequency f, the normalized resonator gain, K_{Res}, is given as

$$K_{Res} = \frac{V_{Dee}(f)}{V_{Dee}(f_H)} = \sqrt{\frac{R_S(f)}{R_S(f_H)}}$$

The highest operating frequency is taken as 27 MHz. The lowest operating frequency is 9.5 MHz for the K1200 and 11 MHz for the K500. A list of the experimental K1200 resonator shunt-impedance values from Vincent's dissertation and the simulated K500 resonator shunt-impedance values from RF Note 116 is given in the following table along with the normalized resonator gain.

Normalized Open-Loop Resonator Gain

Freq. (MHz)	K1200 R_S (kΩ)	K1200 K_{Res}	K500 R_S (kΩ)	K500 K_{Res}
9.5	196.43	1.81		
11	175.13	1.71	98.81	1.45
13	153.09	1.60	89.35	1.38
15	134.19	1.50	80.68	1.31
17	115.92	1.39	72.94	1.25
19	102.47	1.31	66.17	1.19
21	86.95	1.21	60.25	1.13
23	77.87	1.14	55.12	1.08
25	67.19	1.06	50.68	1.04
27	59.69	1.00	46.83	1.00

A graphical representation of this data is given in the following figure:

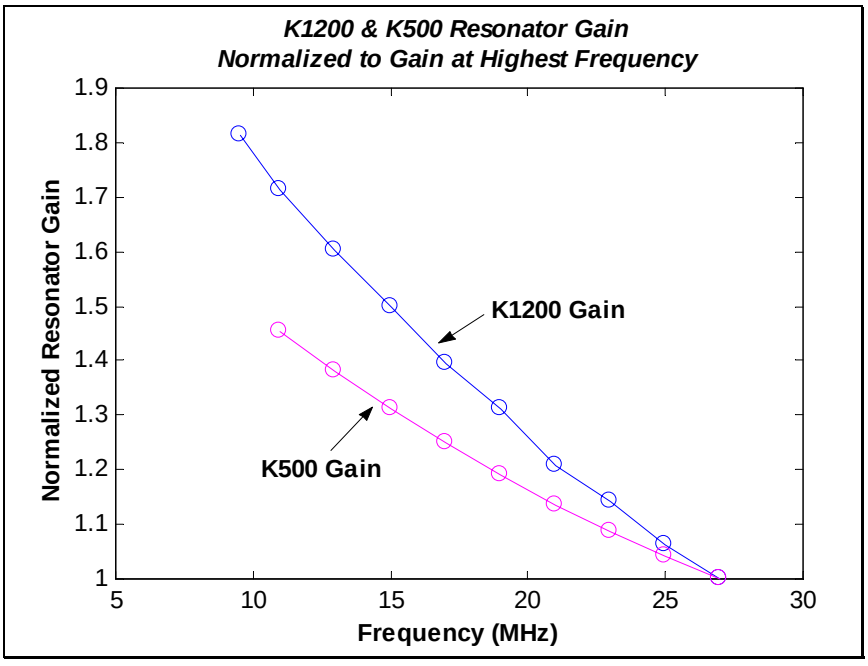

Note: **From the above discussion it is crucial to understand that any change in R_A will result in a change in the resonator open-loop gain. The assumption in this discussion was that R_A is the same at all frequencies. This assumption is violated at the lower RF frequencies due to the range limit on the RF transmitter variable output-coupling capacitor not allowing for a high enough capacitance value. For a detailed discussion of the output-coupling capacitor values see RF Note #117. This violation of the assumption is not of concern since the range limits cause a reduction in open-loop gain through an increase in the tube load-impedance. A reduction in open-loop gain will not effect the closed-loop stability of the voltage-regulation system.**

If R_A is changed by varying the output coupling capacitor, the DVR calibration routine has to redone. DO NOT deviate from the system tuning data for the output coupling capacitor unless all of the tuning data is recalculated AND the DVR calibration routine (in particular setting the full-scale RF output level) is redone.

The Maximum Operating Dee-Voltage

The maximum dee-voltage at which the cyclotron resonators will operate is a function of frequency due to various factors; such as the required voltage for a particular beam, the maximum available power levels attainable from the RF transmitters, and the maximum holding voltage of the resonators before electrical breakdown (arcing) occurs. For a particular beam, the operations group would ideally desire the highest voltage that is attainable. The value which they have asked for currently is 200 KV_{pk} at 26.5 MHz on the K1200 cyclotron. This value happens to be the limit imposed by the RF transmitters. As for electrical breakdown, the maximum holding voltage is mainly influenced by the breakdown voltage of the insulators in the main tuning stems.

The breakdown voltage of the main tuning stem insulators is a fixed number. However, the relationship between the voltage at the insulator and the operating dee-voltage at the median plane is a function of frequency. Thus, the maximum operating dee-voltage is determined as that value of dee-voltage which causes the insulator to be at its breakdown voltage. During the development of the K1200 cyclotron, the breakdown voltage of its insulator was experimentally determined to be 90 KV_{pk}. From the geometry of the insulator region, this was determined to correspond to an electric field of 10.18 KV/cm. This value was determined with the formula for the electric field in a coaxial cable using the inner and outer radii dimensions of the tuning stem at the insulator. In particular the electric field inside a coaxial cable is given as

$$E_{coax} = \frac{V}{r \cdot \ln\left(\frac{b}{a}\right)}$$

where b is the outer radius, a is the inner radius, and r is the radius at which the electric field value is desired. Thus maximum electric field occurs at the inner radius.

Although no experimental data exists for the maximum holding voltage of the K500 insulator region, it will be assumed that the maximum voltage is that voltage which results in the same electric field at the insulator as in the K1200. Using the geometrical dimensions of the K500 main tuning stem, an electric field of 10.18 KV/cm corresponds to 60 KV_{pk} at the insulator. The data used to determine this value is presented in the following table.

Maximum Insulator Voltage of K500 and K1200

Cyclotron	Insulator Inner Radius (cm)	Insulator Outer Radius (cm)	E (KV/cm) at Breakdown	Max Insulator Voltage (KV_{PK})
K1200	32.51	21.59	10.18	90
K500	15.95	23.18	10.18	60

As previously mentioned, the relationship between the dee-voltage and the insulator-voltage is a function of frequency. Thus, the frequency-dependent, maximum dee-

voltage which results in the above maximum insulator voltage (90 KV_{pk} on the K1200, and 60 KV_{pk} on the K500) was determined for the K500 by using John Vincent's circuit simulator, *WAC*, and from previous circuit simulation data for the K1200. The results for both cyclotrons can be found in the following figures. Also included in these graphs is the 200 KV_{pk} limit imposed by the RF transmitters on the K1200 and the 100 KV_{pk} chosen operating limit for the K500.

K1200 Maximum Dee Voltage Data

Freq (MHz)	V_{dee} / $V_{Insulator}$	Dee Voltage (V_{pk}) @Insultor=90KV_{pk}
9	1.10	98.9
11	1.16	104.0
13	1.23	111.1
15	1.34	120.8
17	1.47	132.4
19	1.65	148.8
21	1.92	173.1
23	2.31	207.9
25	2.94	264.3
27	4.25	382.2

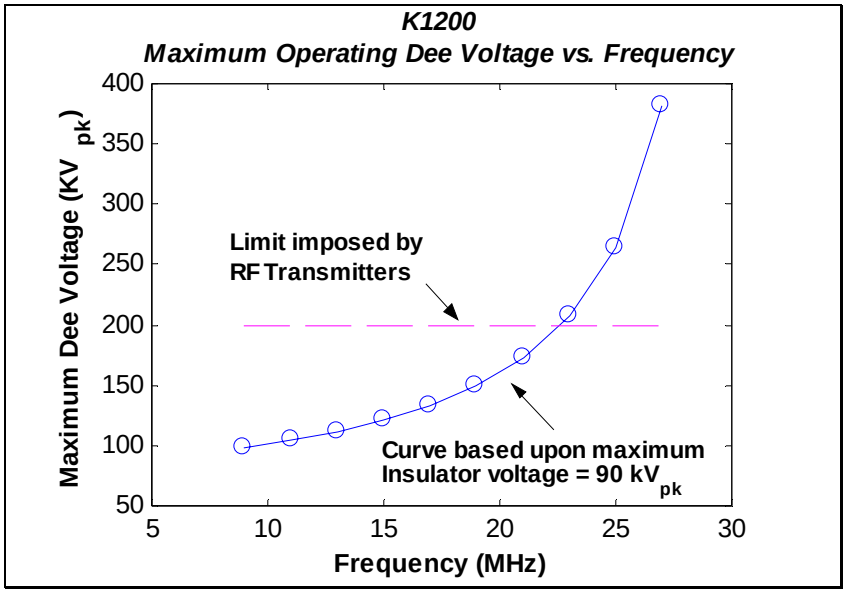

K500 Maximum Dee Voltage Data

Freq (MHz)	V_{dee} / $V_{Insulator}$	Dee Voltage (V_{pk}) @Insultor=90KV_{pk}
11	1.15	68.7
13	1.21	72.7
15	1.30	78.0
17	1.42	85.0
19	1.57	94.3
21	1.78	107.0
23	2.09	125.2
25	2.55	152.9
27	3.32	199.1

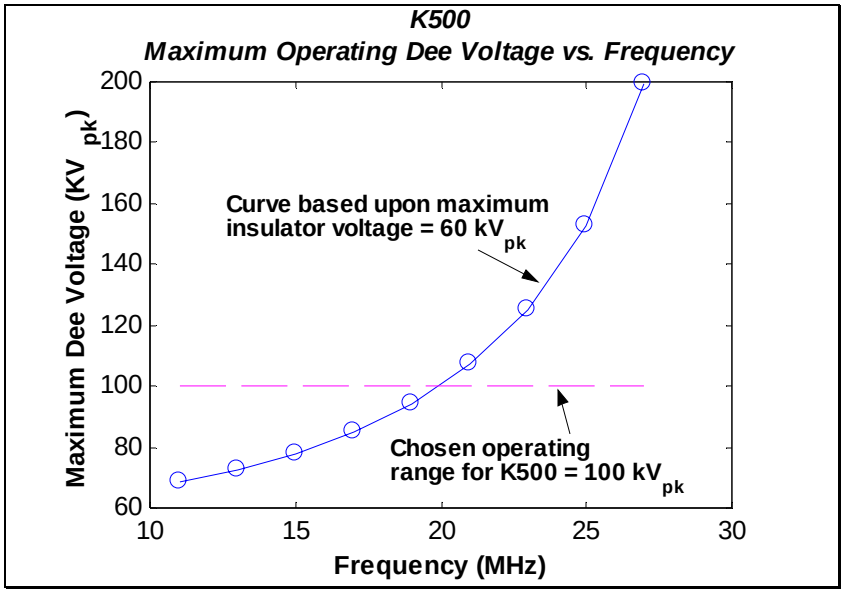

The Experimental Open-Loop Gain

From the above discussions, the open-loop gain of the system is both a function of RF operating frequency and of the operating dee-voltage. In particular as the frequency goes up, the open-loop gain goes down; and as the operating dee-voltage goes up, the gain also goes up. These theoretical predictions were confirmed with experimental measurements on the K1200 during the DVR prototype development. During the experimental investigations a third factor influencing the open-loop gain was found; resonator heating due to operating power levels. As the copper of the resonator heats up, its resistance goes up; causing the effective shunt impedance, and thus the open-loop gain, to go down. The effect is predominantly seen at higher operating RF frequencies since it is at these frequencies that the shunt impedance is already minimum and thus requires more power/heating to begin with. Since closed-loop stability is dictated by the maximum open-loop gain, the design must be stable for the initial cold-gain of the system at the operating points which exhibit this heat-dependence gain.

The experimental data is represented as the gain of the transmitter+resonator, not including the 50Watt amplifier. This format was chosen since the 50Watt amplifiers may easily be replaced in the future with amplifiers that have different gains. Thus, in order to determine the maximum RF output voltage needed from the DVR, this data must be used in conjunction with the gain of the 50Watt amplifiers. Currently, the 50Watt amplifiers on the K1200 cyclotron have a gain of ~47dB corresponding to a voltage gain of ~223.9, while the 50Watt amplifiers on the K500 cyclotron have a gain of ~44dB corresponding to a voltage gain of ~158.5. The actual data acquired from the investigations is tabulated below.

K1200 Transmitter/Resonator Experimental Open-Loop Gain Data

10 MHz			18 MHz			26.5 MHz		
50W Amp Output (V_{pk})	Dee Voltage (KV_{pk})	Gain (KV/V)	50W Amp Output (V_{pk})	Dee Voltage (KV_{pk})	Gain (KV/V)	50W Amp Output (V_{pk})	Dee Voltage (KV_{pk})	Gain (KV/V)
7.25	24.29	3.35	7.20	18.50	2.57	7.35	10.00	1.36
8.94	30.80	3.45	9.87	27.20	2.76	12.39	20.00	1.61
12.26	46.80	3.82	12.63	38.50	3.05	16.05	30.00	1.87
15.63	68.94	4.41	15.37	52.90	3.44	19.09	40.00	2.10
17.01	80.00	4.70	18.06	70.00	3.88	21.50	50.00	2.33
18.14	90.00	4.96	20.70	91.00	4.40	23.76	60.00	2.53
18.70	95.00	5.08	19.40	80.00	4.12	25.74	70.00	2.72
			21.72	100.00	4.60	27.78	80.00	2.88
			22.91	111.00	4.85	29.63	90.00	3.04
			23.75	120.00	5.05	31.49	100.00	3.18
			24.75	129.00	5.21	33.80	110.00	3.25
			24.89	130.00	5.22	36.35	120.00	3.30
			26.02	140.00	5.38	39.09	130.00	3.33
						42.09	140.00	3.33

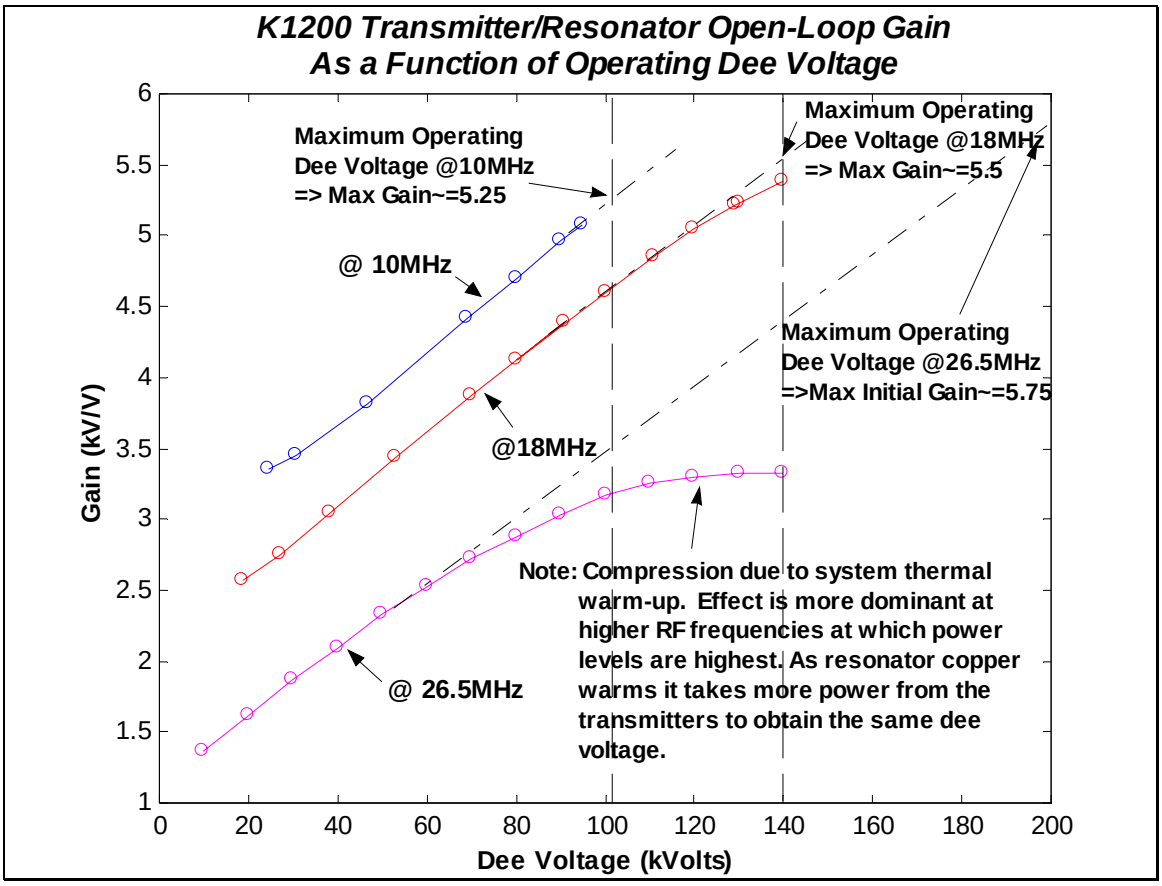

The above experimental graph displays all of the above mentioned factors which influence the open-loop gain. At each frequency, the increase in gain with increasing dee-voltage, due to the RF transmitter tube, is clearly evident. Furthermore, the decrease in gain as a function of RF frequency, due to the decrease in shunt impedance, is also confirmed. Furthermore, the decrease in gain as a function of heating is clearly seen in the slight compression of the 18 MHz data and the larger compression in the 26.5 MHz data. And finally, the above graph displays the frequency-dependent, maximum operating dee-voltage data that was calculated based upon the insulator breakdown-voltage.

As could be deduced from the theoretical discussions of these factors which influence the gain, the factors would ideally almost null each other out due to the combination of 1.) the increasing gain with increasing dee-voltage, and 2.) the decreasing gain as a function of RF frequency coupled with the increase in maximum operating dee-voltage as a function of frequency. This nulling effect is seen in the experimental data if the resonator heating effect is ignored. Looking at the dashed lines extrapolated along the lines of data, in conjunction with the maximum operating dee-voltage, the maximum open-loop gain for all frequencies would be almost identical at approximately 5.5 KV/V. Without the heating effect, the closed loop design would not have to take into account any increase in open-loop gain as the RF frequency was decreased.

However, as seen from the data, the compression due to resonator heating forces the maximum open-loop gain to be roughly only 3.25 KV/V at the maximum operating dee-voltage for 26.5 MHz. This value forces the full-scale RF output level needed from the DVR to be that voltage which will result in $\frac{200\,KV_{pk}}{\sqrt{2}\cdot 3.25\,KV/V} = 43.5\,V_{RMS}$ from the 50Watt amplifier. This is equivalent to 37.8 Watts into 50 Ohms, a value which closely correlates to the known 50Watt amplifier power level needed for operating at 26.5 MHz.

This full-scale 50W-amp output level sets the high-frequency gain from which the system gain at lower RF frequencies can be determined. Selecting this full-scale level is the crucial step in generating the actual curve of open-loop gain versus RF frequency. The importance of this step becomes quite evident when designing the closed-loop system as will be discussed later. For now, it is interesting to note the following:

Note: ***Choosing the full-scale 50W-amp RF output level to result in the maximum dee-voltage at 27MHz (V_{max}@27MHz) forces the 0-10v DVR command voltage to correspond to 0-V_{max}@27MHz. At lower RF frequencies, where the open-loop gain is higher, 0-10v to the DVR will correspond to a dee-voltage much higher than V_{max}@27MHz. This increase in open-loop gain will effect the closed-loop design. The details of the effects will be discussed in the closed-loop design section of this RF note.***

Note, however, that the change in open-loop gain does not alter the fact that a 0-10v command will always correspond to 0-$V_{Full\text{-}Scale}$ in closed-loop (where $V_{Full\text{-}Scale}$ is the chosen full-scale range: 200kV_{pk} on the K1200, and 100kV_{pk} on the K500). The feedback attenuator-scalings are ultimately chosen such that 0-10v corresponds to this 0- $V_{Full\text{-}Scale}$. Thus, when the closed-loop design regulates the system for zero-error, the command-to-dee-voltage scaling will remain fixed. It is only the open-loop gain and the closed-loop dynamics which are affected by the effects previously discussed.

Overview of the Transmitter/Resonator Open-Loop Gain Discussion

This sub-section is intended to give a brief overview of the open-loop gain topics discussed and the results achieved from that discussion. Instead of having to search through the previous discussions, all results are summarized here.

The purpose of the open-loop gain discussion was to provide the maximum open-loop gain constants which the closed-loop design would have to consider. The previous graph of the K1200 experimental gain represents all the information needed to generate a table of the maximum open-loop gain versus RF frequency. This graph could have been created using the theoretical data accumulated from the discussions of the factors effecting the open-loop gain. In fact, an equivalent graph is needed for the K500. In the process of generating a theoretical graph for the K500, the theoretical K1200 graph will also be generated. These graphs are the ultimate piece of open-loop gain information needed for the closed-loop design.

In order to generate the theoretical curves of open-loop gain vs. RF frequency and dee-voltage, the following considerations must taken into account.

1.) The load impedance, R_A, presented to the anode of the transmitter's TH555 tube fixes the maximum anode voltage swing before screen-conduction and also fixes the resonator gain according to the formula:

$$K_{\mathrm{Re}s}(f) = \frac{V_{Dee}}{V_A} = \sqrt{\frac{R_S(f)}{R_A}},$$

where V_A is the anode voltage, V_{Dee} is the dee-voltage, and $R_S(f)$ is the resonator shunt-impedance at frequency f. R_A is typically chosen based upon the desired efficiency of operation at the maximum operating power-level (usually highest-RF frequency) in conjuction with the anode bias-power-supply specifications. It is usually set experimentally during system conditioning/mapping. It's exact value is not critical since it is the variation in gain that is of concern.

2.) The resonator open-loop gain is a function of frequency due to the resonator shunt-impedance. Normalizing all gains to the gain at the highest RF frequency results in a normalized gain expression of:

$$K_{Normalized} = \frac{V_{Dee}(f)}{V_{Dee}(f_H)} = \sqrt{\frac{R_S(f)}{R_S(f_H)}},$$

where $R_S(f_H)$ is the shunt impedance at the highest RF frequency (27MHz for both the K500 and the K1200). Due to the decrease in shunt-impedance as the frequency increases, the normalized gain will start at its max at the lowest frequency and decrease down to unity at the highest frequency. Thus, determine the normalized gain as a function of RF frequency using the resonator shunt-impedance values.

3.) Assume that the transmitter-gain changes as a function of anode-voltage according to the graph generated from the TH555 circuit simulations (see *The Transmitter Open-Loop Gain* section). Normalize the transmitter-gain at the highest anode-voltage, since this is the maximum transmitter-gain, and maximum transmitter output-power.

4.) The maximum operating dee-voltage as a function of frequency is determined from the maximum inulator voltage before breakdown. This maximum operating voltage places a limit on the maximum system gain as a function of frequency.

5.) The maximum full-scale RF level needed from the 50W-amp is determined as that amount of RF that is needed to bring the system to the maximum dee-voltage at 27MHz ($200kV_{pk}$ on the K1200, and $100kV_{pk}$ on the K500). This sets the open-loop gain to unity at 27MHz.

6.) The full-scale RF level needed from the DVR is determined from the gain of the 50W-amp in conjunction with the RF level from step 5.

7.) The maximum open-loop gain as a function of frequency is thus determined from the combination of the above steps.

The actual steps used to generate the theoretical curves are as follows:

1.) Start with 27MHz. Find the Power needed for V_{Dee} max ($100kV_{pk}$ on K500, $200kV_{pk}$ on K1200) using the shunt-impedance.
2.) Find a value for R_A assuming that V_A max is $17kV_{pk}$ from $R_A \cong (17kV)^2 / (2 \cdot P_{max})$
3.) Find the gain vs. dee-voltage at 27MHz using the TH555 gain curve. This assumes that a change in V_A by a factor of $2000/17000 = 0.118$ results in a gain change by a factor of $20/45 = 0.44$. Normalize all gains such that the open-loop gain is unity for V_{Dee} max at 27MHz. Thus, the transmitter gain is given as $G = \frac{0.635}{V_A \max} \cdot V_A + 0.365$
4.) Now, at any other frequency, find the maximum operating dee-voltage on the curve generated from the insulator breakdown voltage. At this max dee-voltage, determine the tube anode-voltage, V_A, from the resonator shunt-impedance and the R_A value from step 2.
5.) Find the ratio between V_A determined in step 4 and the V_A max value of $17kV_{pk}$ as $ratio = V_A / 17kV$.
6.) Using the ratio from step 5, find the transmitter gain from the gain equation in step 3 using $V_A = ratio \cdot V_A \max$.
7.) Now, find the increase in gain due to the change in shunt-impedance at this new frequency. Multiply the gain found in step 6 by $\sqrt{R_S(f) / R_S(27MHz)}$.
8.) Repeat steps 4-7 for various dee-voltages and RF frequencies to generate the entire family of gain-curves.

The theoretical curves for both the K500 and the K1200 are shown on the following page.

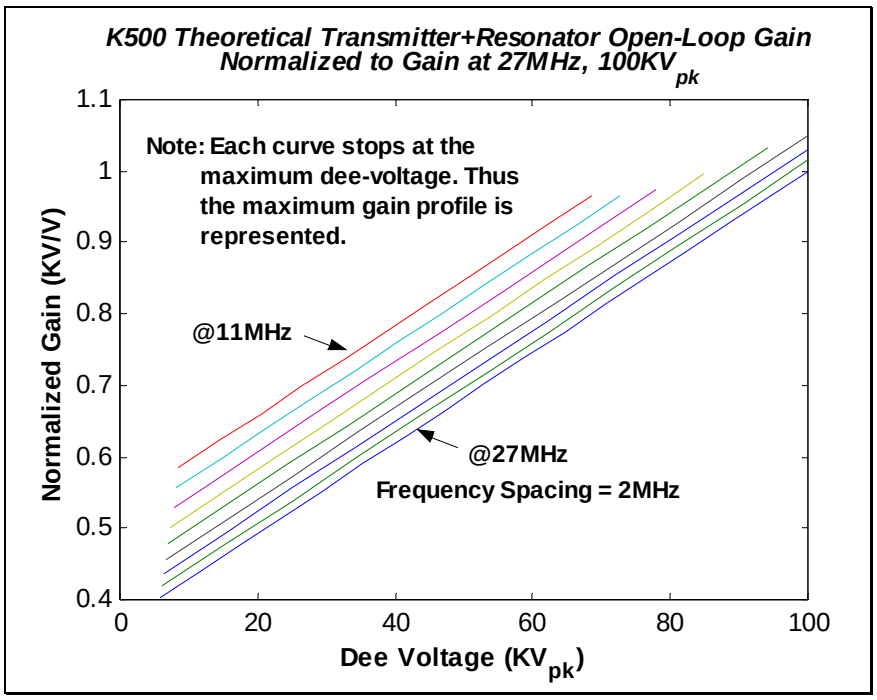

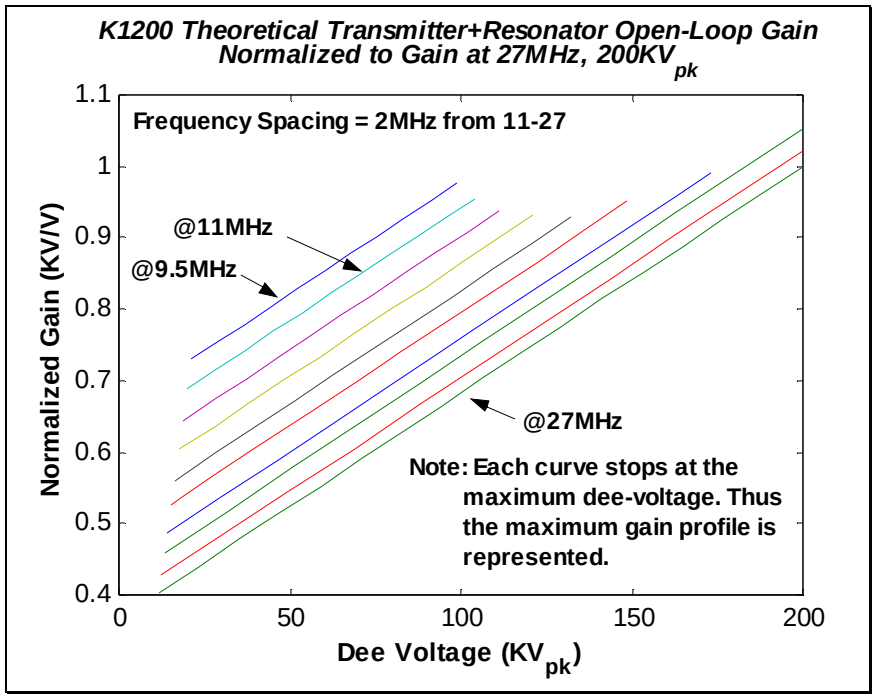

Note: ***These curves do not include any decrease in shunt-impedance due to resonator heating (the gain-compression at higher frequencies and higher dee-voltages). These theoretical curves correlate quite well with the experimental K1200 curves. They also nicely represent the maximum gain profile which is mainly influenced by the maximum dee-voltage in conjunction with the shunt-impedance. The maximum dee-voltage on the K500 and the K1200 curves is limited to $100KV_{pk}$ and $200KV_{pk}$ respectively.***

The RF Peak Detector

The RF peak-detector is the feedback sensing element for the RF voltage regulation system. It is the most crucial element since it gives the regulation system a measurement of the dee-voltage. A block diagram of the peak-detector design is shown below:

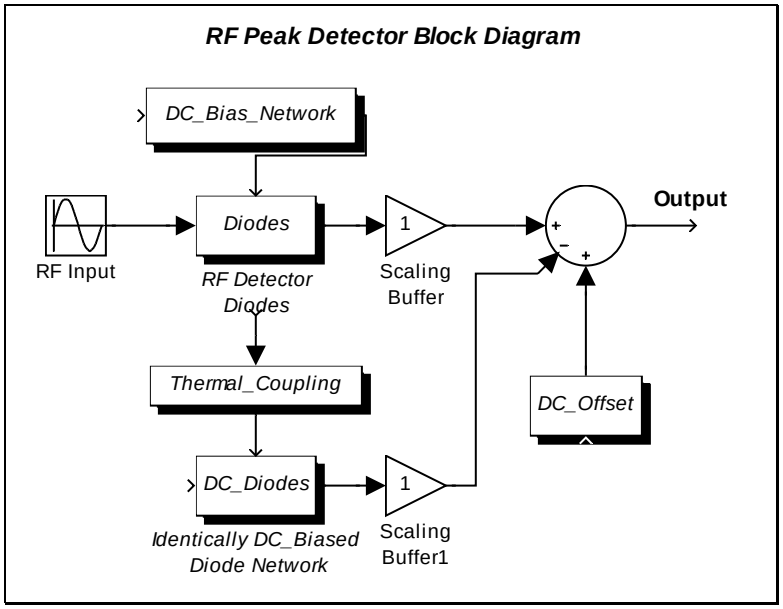

RF Peak Detector Block Diagram

A DC-bias was applied to the detector-diodes to increase the sensitivity of the diodes to RF voltage levels. Since this DC-bias appears at the output of the detector-diodes' buffer amp, the output-summer subtracts this DC-bias using an identically biased diode-network. The detector-diodes and the identically biased diodes are physically touching each other, creating a thermal coupling between the two so as to eliminate any output drift due to temperature changes. Finally, a DC-offset voltage is added to the output to increase the accuracy of the device. This offset-voltage will be discussed later in detail.

The actual circuit schematic is shown in full detail on the following page.

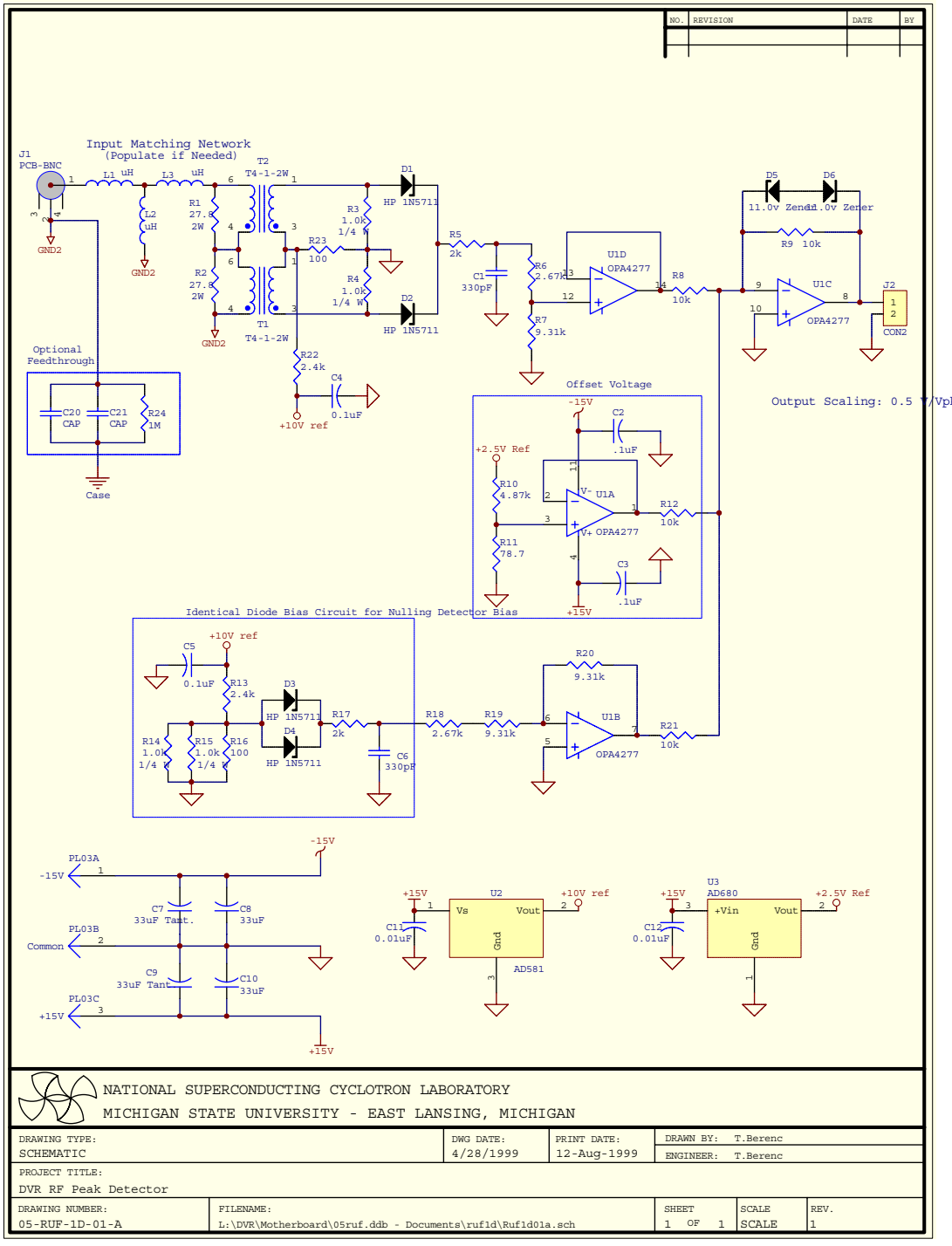
NO. REVISION DATE BY
Input Matching Network
(Populate if Needed)
J1
PCB-BNC
L1 uH
L3 uH
L2 uH
T2
T4-1-2W
T1
T4-1-2W
R1 27.8 2W
R2 27.8 2W
R3 1.0k 1/4 W
R4 1.0k 1/4 W
R23 100
R22 2.4k
C4 0.1uF
+10V ref
D1
HP 1N5711
D2
HP 1N5711
R5 2k
C1 330pF
R6 2.67k
R7 9.31k
U1D
OPA4277
R8 10k
D5
D6
11.0v Zener
11.0v Zener
R9 10k
U1C
OPA4277
J2
CON2
Output Scaling: 0.5 V/Vpk
GND2
Optional Feedthrough
C20 CAP
C21 CAP
R24 1M
Case
Offset Voltage
-15V
C2 .1uF
+2.5V Ref
R10 4.87k
R11 78.7
U1A
OPA4277
R12 10k
C3 .1uF
+15V
Identical Diode Bias Circuit for Nulling Detector Bias
+10V ref
C5 0.1uF
R13 2.4k
R14 1.0k 1/4 W
R15 1.0k 1/4 W
R16 100
D3
HP 1N5711
D4
HP 1N5711
R17 2k
C6 330pF
R18 2.67k
R19 9.31k
R20 9.31k
U1B
OPA4277
R21 10k
PL03A
-15V
PL03B
Common
PL03C
+15V
C7 33uF Tant.
C8 33uF
C9 33uF Tant.
C10 33uF
+15V
U2
Vs
Vout
Gnd
AD581
C11 0.01uF
+10V ref
U3
AD680
+Vin
Vout
Gnd
C12 0.01uF
+2.5V Ref
NATIONAL SUPERCONDUCTING CYCLOTRON LABORATORY
MICHIGAN STATE UNIVERSITY - EAST LANSING, MICHIGAN
DRAWING TYPE: SCHEMATIC
DWG DATE: 4/28/1999
PRINT DATE: 12-Aug-1999
DRAWN BY: T.Berenc
ENGINEER: T.Berenc
PROJECT TITLE: DVR RF Peak Detector
DRAWING NUMBER: 05-RUF-1D-01-A
FILENAME: L:\DVR\Motherboard\05ruf.ddb - Documents\ruf1d\Ruf1d01a.sch
SHEET 1 OF 1
SCALE SCALE
REV. 1

The RF Input Operating Range

The RF input frequency range specification for the peak-detector was set by the cyclotron operating frequency range. 9MHz-27MHz. The RF input voltage range specification was set by the combination of the cyclotron dee-voltage operating range, the RF frequency operating range, and the dee-stem pickup-loop scaling factors, which are cyclotron dependent.

To determine the RF input voltage range, the dee-voltage pickup-loop scaling factors are needed. The K500 and K1200 scaling factors are listed in the following table. The K500 scaling factors are the experimentally-adjusted, theoretical scaling factor table from RF Note 119. The K1200 scaling factors are from John Vincent's dissertation.

K500 & K1200 Dee-Voltage Pickup-Loop Scaling Factors Used for DVR Design

Frequency (MHz)	K500 Pickup-Loop Scaling Factor (KV/V)	K1200 Pickup-Loop Scaling Factor (KV/V)
9.5		62.83
11	28.69	50.43
13	21.88	38.59
15	17.21	30.65
17	13.99	25.28
19	11.64	21.07
21	9.90	18.03
23	8.57	15.33
25	7.55	12.59
26.5	~6.94	11.48
27	6.74	~11.20

During the DVR development, the pickup-loop scaling factor was measured using the current K1200 DVR readout (with the RF tune-data attenuator settings) and the same Fluke RF peak-detector probe used on the K500 investigations. At 18MHz and 26.5MHz, the measured scaling factors correlated quite well with values from Vincent's dissertation. However, the scaling factor at 10MHz measured a lot lower than Vincent's value. In order to investigate the discrepancy at 10MHz, X-ray data from January of 1999 was reviewed. X-ray data did exist for 18MHz and 26.5MHz, however no x-rays were able to be measured at 10MHz, thus the data accumulated for 10MHz had used the same attenuator settings from the RF tune data that were used for the DVR development. For the rest of the pickup-loop scaling factor discussion in this note, the K1200 scaling factors will be taken from Vincent's dissertation. The developmental investigations are documented in the following table for reference.

K1200 Scaling Factor Investigations during DVR Development

Frequency (MHz)	DVR Reading (KV_{pk})	Fluke Probe (V_{pk})	Measured Scaling Factor (KV/V)	Vincent's Scaling Factor (KV/V)
10	60	1.24	48.38	60.08
18	115.2	4.32	26.67	23.18
26.5	130	10.38	12.52	11.48

From the *K500 & K1200 Dee-Voltage Pickup-Loop Scaling Factor* table, the RF input voltage range can be calculated. It is assumed that the maximum operating dee-voltage is $100KV_{pk}$ for the K500 and $200KV_{pk}$ for the K1200. Thus, the maximum RF input voltage to the RF peak-detector will occur with this maximum dee-voltage at 27MHz. The minimum RF input voltage to the RF peak-detector will occur with the lowest dee-voltage at the lowest RF frequency (11MHz for the K500, 9.5MHz for the K1200). It will be assumed that the lowest operating dee-voltage is $20KV_{pk}$ for the K500 and $30KV_{pk}$ for the K1200. The minimum and maximum RF input voltages to the peak-detector are tabulated below:

Operating Input Voltage Range to Peak-Detector

Cyclotron	Minimum RF Input (V_{pk})	Maximum RF Input (V_{pk})
K500	0.70	14.84
K1200	0.64	17.86

Chosen Peak Detector Input Range: 0.0 – $20V_{pk}$

Chosen Peak-Detector Scaling: 0.5 VDC per 1 V_{pk} RF

The peak-detector input voltage-range was chosen to be 0.0 - $20V_{pk}$. $20V_{pk}$ corresponds to 4Watts into 50Ω. This power-level forced the design to use two 2Watt RF transformers from Mini-Circuits. These RF transformers were connected in series as shown in the circuit-schematic. The proper way to connect these transformers in series was to also connect two series resistors in parallel with the primary side of the transformers with the common connection tied to the common connection of the transformers (see the schematic for details). This layout forced the RF voltage across each transformer to be identical, thereby reducing effects caused from any imbalances between the transformers.

Based upon the chosen input voltage-range, the scaling factor relating the DC output of the peak-detector to the RF input-voltage was chosen to be 0.5 VDC per 1 V_{pk} RF. Thus 0.0 - $20V_{pk}$ RF corresponds to 0 – 10.0 VDC.

The DC-Bias on the Detector-Diodes

The diodes chosen for the peak-detector design were the Hewlett-Packard (HP) 1N5711 Schottky-barrier diodes. They were chosen both for their low turn-on voltage of 0.41V and for their high reverse breakdown voltage of 70V. Although the turn-on voltage is considerably low, it is still close to the minimum level of peak RF voltage as determined above in the *RF Input Operating Range* section. Thus, a dc-bias was designed into the peak-detector in order to increase its accuracy at these low RF input levels.

An experimental comparison of the peak-detector design with and without the dc-bias was measured at 15MHz RF. The results can be found in the following graph:

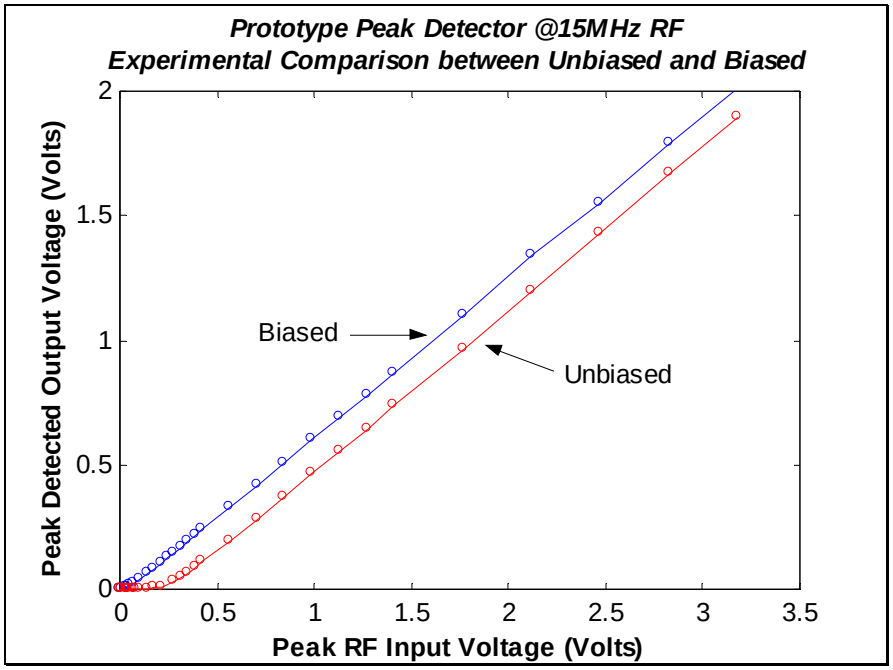

The advantage of the dc-bias is quite evident. In fact the threshold at which the peak-detector begins to detect occurs at roughly $30mV_{pk}$ of RF with the dc-bias as compared to $250mV_{pk}$ of RF without the dc-bias.

The DC-Offset Voltage

The need for the dc-offset voltage becomes apparent from the purpose of the peak-detector as an instrument. The ideal peak-detector instrument would output a voltage that was a directly proportional to the RF input voltage; such as $0.0 – 20.0V_{pk}$ RF corresponding to 0 – 10.0VDC. This relationship would result in a simple scaling ratio of 0.5 VDC/$V_{pk\ RF}$. Thus, to use the peak-detector as an RF voltage measuring instrument, one would simply multiply the DC output by 2 to obtain the RF voltage level at the input of the peak-detector.

The actual peak-detector is not that simple. The reason is due to the detector threshold, the RF level at which the peak-detector begins to detect. This threshold is a result of the non-zero turn-on voltage of the detector diodes.

To better understand this discussion, let us look at a graph of the RF input level vs. peak-detected output. This is the inverse function of the previous graph showing the comparison between the biased and unbiased detector. The reason for using the inverse function is that this is truly how the peak-detector will be used as an instrument. In particular, the DC-output of the peak-detector will be translated into a corresponding RF input voltage. The discussion will refer to the following graph:

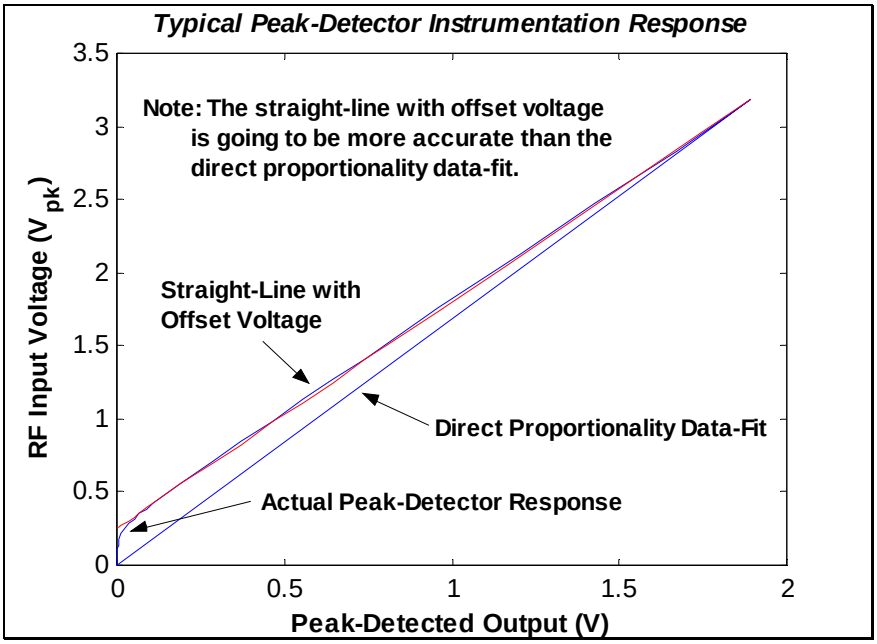

As can be seen from the graph, a direct proportionality relationship between the peak-detected output and the RF input voltage does not accurately predict the actual RF input voltage. Of course, the slope (or proportionality constant) could be altered to balance the error between the low-levels and high-levels, but it still will not be as accurate as a straight-line fit with a y-intercept.

The following figure gives the percent error of both types of data fits with respect to the actual peak-detector response. This percent error is calculated as the percent error between the RF-input voltage predicted by the fit and the actual RF-input voltage. It is a classical percent error calculation as given by

$$\%Error = \frac{predicted - actual}{actual} \cdot 100\%,$$

as opposed to a percent error with respect to full scale. I point this out because a lot of data sheets these days give the percent error with respect to full scale; a measure that does not tell the exact accuracy of the measuring device at a particular level, rather it is more of a resolution-type measurement that makes the %error numbers smaller and thus more attractive.

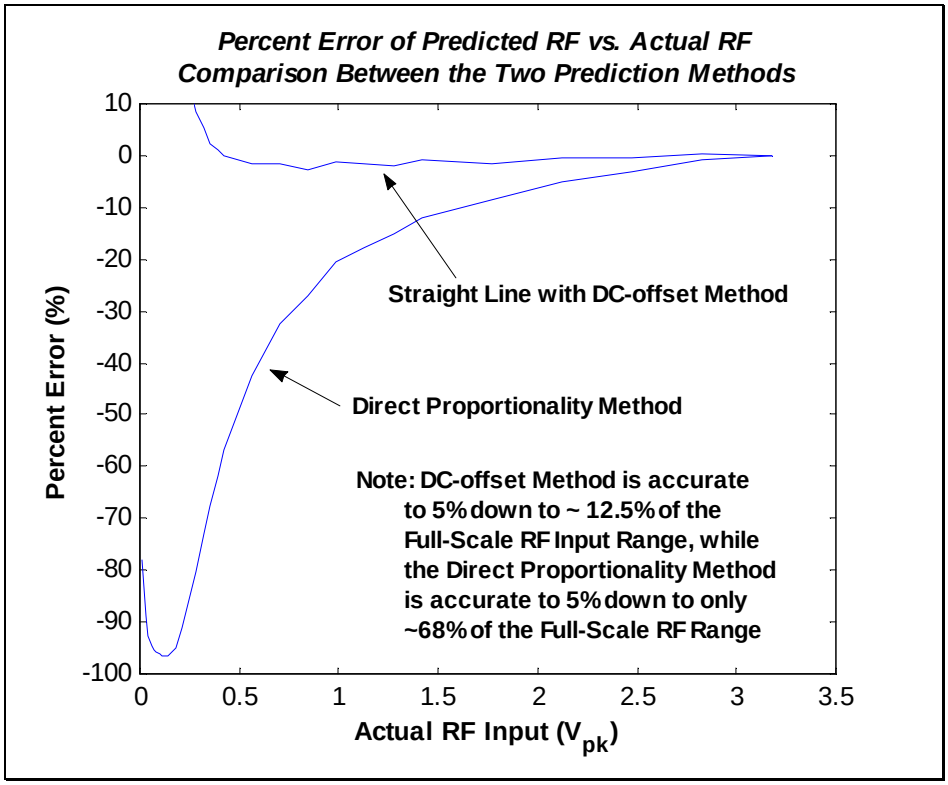

Clearly, the straight-line with a DC-offset prediction curve is more accurate across a larger portion of the RF-input range than the direct-proportionality prediction curve.

The previous discussion clarifies the need for the offset voltage, but it does not discuss the subtleties that arise in actually implementing the DC-offset voltage within the DVR module.

It has already been seen that the optimum first-order function for predicting the RF-input level based upon the peak-detector's output is a straight line with a y-intercept in the form of:

$$RF\ \ Input = m \cdot (RF\ \ Peak\ \ Detector\ \ Output) + (yIntercept)$$

As stated previously, the ideal instrumentation device would predict the RF-input level based upon a direct proportionality between its input and output such as:

$$RF\ \ Input = Scaling \cdot (DeviceOutput)$$

Thus, equating the above two equations, an equation for the device output is derived as

$$DeviceOutput = \frac{m}{Scaling} \cdot (RF\ \ Peak\ \ Detector\ \ Output) + \frac{(yIntercept)}{Scaling}$$

This is the equation which was used to design the complete RF peak-detector with the DC-offset. Referring back to the peak-detector block-diagram, the summing junction represents the above equation. (Keep in mind that the subtracted input of the summing junction represents the nulling of the diode dc-bias and thus does not affect the above equations). Clearly, the DC-offset is given as the second term of the right-hand side:

$$DC\ Offset = \frac{(yIntercept)}{Scaling}\ .$$

Notice that in the block diagram, there is a unity buffer amp that feeds the RF peak-detector output into the summing junction. Thus it appears that the $(m / Scaling)$ factor from the *DeviceOutput* equation is not being applied. It so happened that in this case m and $Scaling$ were approximately equal to each other. This will be seen later when the experimental output responses are presented.

As a stand-alone instrument, adding the DC-offset voltage right on the peak-detector board optimizes the accuracy of the RF-peak detector.

The Experimental Peak-Detector Output Response

During development of the RF peak-detector, experimental measurements were performed simultaneously on two identical peak-detector boards. This provided both experimental response curves for the peak-detector itself, and measurements of the repeatability of the design from unit-to-unit. The measurements were performed over the entire RF-input voltage range ($0.0 – 20V_{pk}$) for three different frequencies, 10MHz, 18MHz, and 26.5Mhz. The measurements are tabulated below and are displayed in the figure proceeding the table.

Peak Detector Final Design Experimental Measurements

10MHz			18MHz			26MHz		
RF Input (V_{pk})	Serial #1 (V)	Serial #2 (V)	RF Input (V_{pk})	Serial #1 (V)	Serial #2 (V)	RF Input (V_{pk})	Serial #1 (V)	Serial #2 (V)
0.000	0.041	0.040	0.000	0.039	0.040	0.000	0.040	0.040
0.102	0.066	0.067	0.102	0.067	0.068	0.100	0.067	0.068
0.201	0.108	0.109	0.200	0.111	0.112	0.200	0.112	0.112
0.300	0.152	0.153	0.300	0.158	0.159	0.600	0.160	0.159
0.400	0.196	0.197	0.400	0.203	0.205	0.401	0.206	0.208
0.503	0.243	0.244	0.501	0.252	0.253	0.501	0.256	0.257
1.000	0.469	0.470	1.000	0.490	0.492	1.002	0.498	0.501
2.010	0.960	0.962	2.000	0.997	1.003	2.000	1.013	1.021
6.010	1.448	1.453	3.000	1.508	1.517	3.010	1.537	1.547
4.005	1.915	1.916	4.015	2.009	2.023	4.015	2.032	2.039
5.005	2.405	2.408	5.020	2.517	2.533	4.995	2.533	2.547
6.265	3.016	3.013	6.265	3.159	3.182	6.250	3.185	3.204
7.495	3.626	3.630	7.520	3.810	3.837	7.520	3.842	3.866
8.755	4.189	4.194	8.755	4.408	4.442	8.750	4.413	4.446
10.000	4.785	4.792	10.000	5.036	5.073	10.005	5.049	5.083
11.275	5.410	5.420	11.255	5.692	5.738	11.285	5.702	5.742
12.525	6.025	6.031	12.525	6.373	6.424	12.530	6.358	6.400
15.010	7.297	7.310	15.030	7.685	7.750	15.030	7.678	7.734
17.500	8.546	8.569	17.520	9.022	9.115	17.550	8.994	9.123
20.100	9.760	9.796	20.000	10.300	10.394	20.000	10.267	10.462

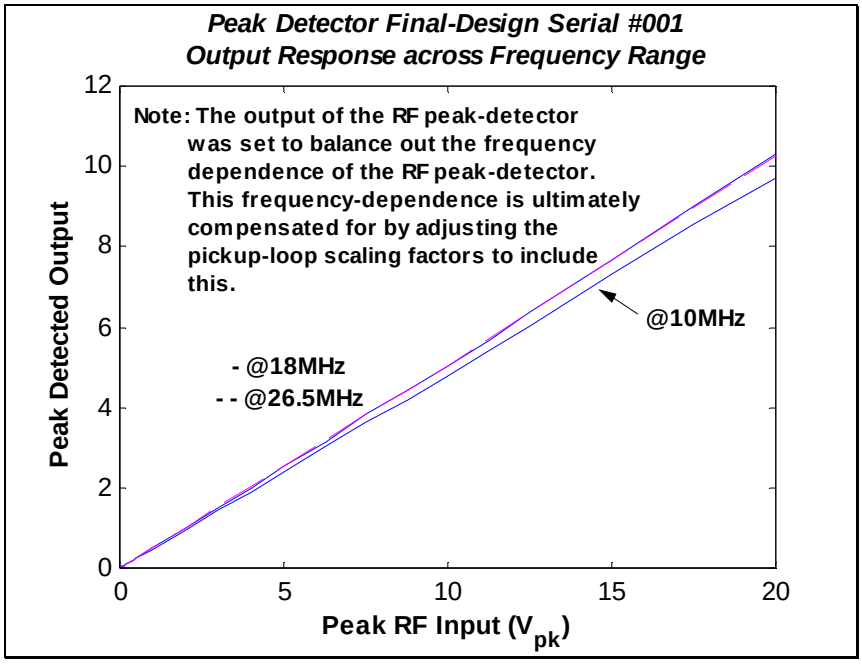
Peak Detector Final-Design Serial #001
Output Response across Frequency Range
Note: The output of the RF peak-detector was set to balance out the frequency dependence of the RF peak-detector. This frequency-dependence is ultimately compensated for by adjusting the pickup-loop scaling factors to include this.
@10MHz
- @18MHz
- - @26.5MHz
Peak Detected Output
Peak RF Input (Vpk)
0
2
4
6
8
10
12
0
5
10
15
20

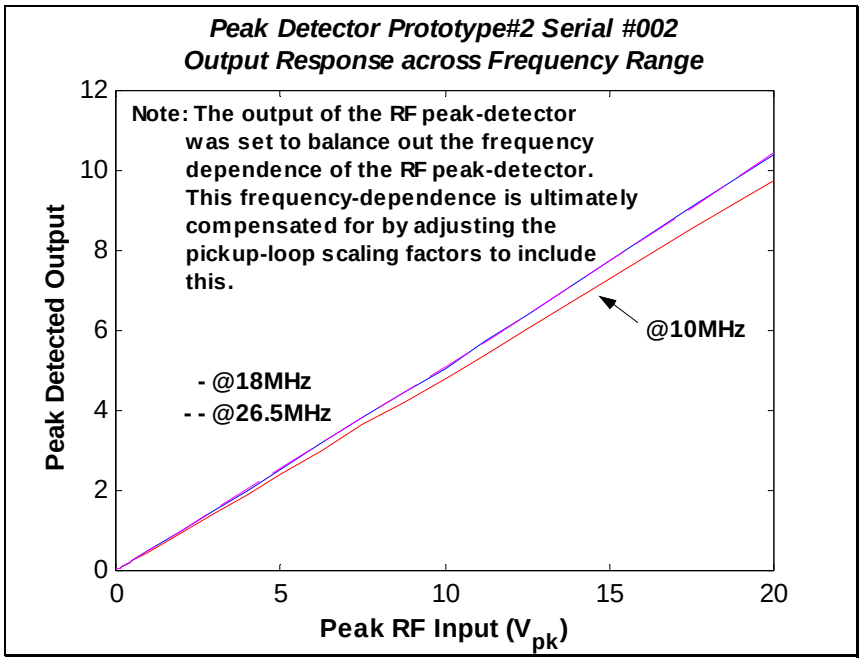
Peak Detector Prototype#2 Serial #002
Output Response across Frequency Range
Note: The output of the RF peak-detector was set to balance out the frequency dependence of the RF peak-detector. This frequency-dependence is ultimately compensated for by adjusting the pickup-loop scaling factors to include this.
@10MHz
- @18MHz
- - @26.5MHz
Peak Detected Output
Peak RF Input (Vpk)
0
2
4
6
8
10
12
0
5
10
15
20

The repeatability of the peak-detector from unit-to-unit is a measure of interest. This was performed by measuring the percent difference of serial#002 with respect to serial#001. The resultant graph is shown below:

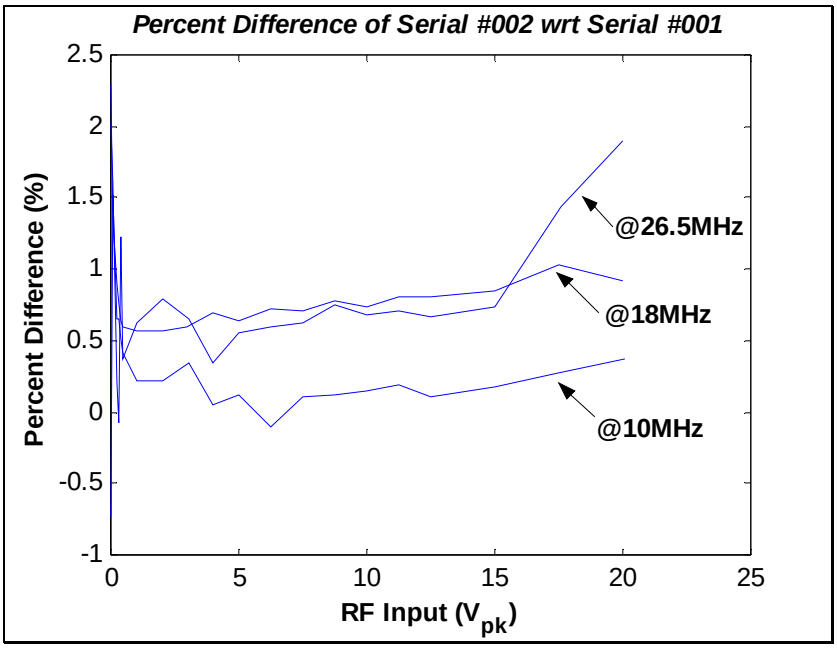

It is evident from the graph that the peak-detectors agree with each other well within 0.5% at 10MHz, 1% at 18MHz, and 2% at 26.5MHz.

The Peak-Detector Frequency-Dependence Factor

As seen from the output response plots, the peak-detector does has a slight frequency dependence. This is believed to be due to the RF transformers and not the peak-detector diodes. The design balanced the frequency-dependence such that the average output of the peak-detector was 10.0V at $20V_{pk}$ of RF.

This frequency-dependence does have to be taken into account when determining the attenuator values. This is done by including the peak-detector frequency-dependence into the pickup-loop scaling factors. The additional scaling-factor from the peak-detector was calculated by finding the term that would force the peak-detector output to 10.0V at $20V_{pk}$ of RF for each frequency.

The additional pickup-loop gain term introduced through the peak-detector is plotted in the following graph. The actual data values are given in the table proceeding the graph. This data includes interpolated values from a straight-line fit to the data accumulated from the experimental responses at 10MHz, 18MHz, and 26.5MHz.

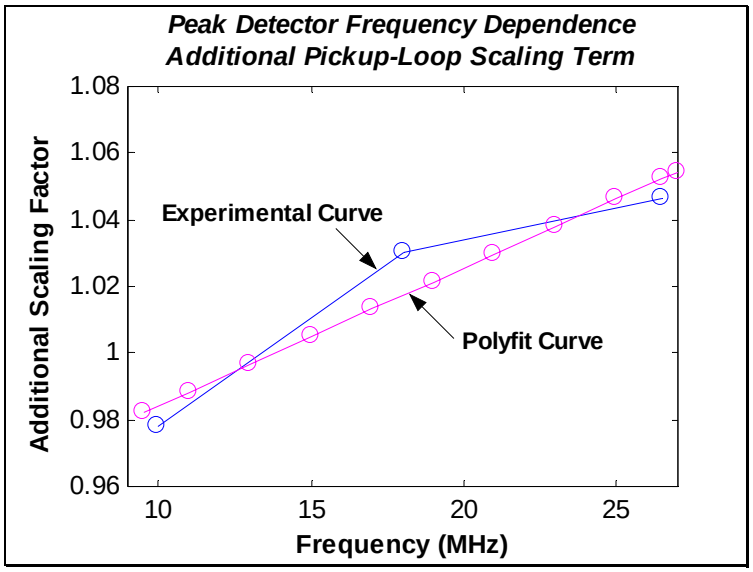

Additional Pickup-Loop Scaling Introduced by Peak-Detector

Frequency (MHz)	Experimental Scaling Factor	Polyfit Scaling Factor
9.5		0.982
10	0.978	
11		0.988
13		0.997
15		1.005
17		1.013
18	1.030	
19		1.021
21		1.030
23		1.038
25		1.046
26.5	1.046	1.052
27		1.054

Temperature Drift Measurements

Another characteristic of interest is the temperature-dependence of the peak-detector. This was measured by placing the peak-detector in an oven and measuring its DC output level as a function of temperature. These measurements were taken at an RF operating frequency of 18MHz with 4 levels of RF-input ($0.5V_{rms}$, $1V_{rms}$, $5V_{rms}$, and $13.8V_{rms}$). The results are shown below. The data used to derive the results can be found following the graph.

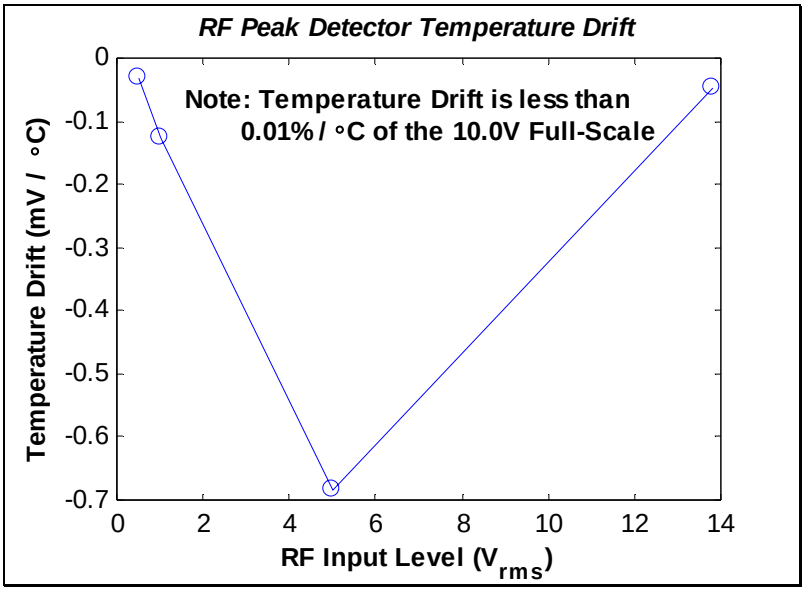

Peak-Detector Temperature Drift Data

RF In = 0.5 V_{rms}		RF In = 1 V_{rms}		RF In = 5 V_{rms}		RF In = 13.8 V_{rms}	
Temp (C)	Output (V)	Temp (C)	Output (V)	Temp (C)	Output (V)	Temp (C)	Output (V)
24.3	0.361	30.6	0.718	26.7	3.663	35.0	9.594
40.6	0.359	35.0	0.717	29.4	3.661	38.3	9.595
46.1	0.360	37.8	0.716	32.2	3.658	51.7	9.595
48.9	0.360	40.6	0.716	35.0	3.657	56.1	9.593
54.4	0.360	43.3	0.716	37.8	3.655		
		48.9	0.716	40.6	3.654		
		54.4	0.715	43.3	3.652		
				46.4	3.649		
				48.9	3.647		
				51.7	3.645		
				54.4	3.644		

The Motherboard Attenuator

Ultimately the DVR correlates a 0-10.0V command signal into a 0-V_{DeeMax} dee-voltage. It does this by expecting a feedback signal with the same proportional relationship. Thus, the feedback signal should correlate 0-V_{DeeMax} into 0-10.0V.

All would be well if a dee-voltage of V_{DeeMax} resulted in $20V_{pk}$ of RF to the input of the peak-detector since the peak-detector is designed to give 0.5 VDC per $1V_{pk}$ of RF. However, this is not the case. Due to the dee-voltage pickup-loop scaling factors, a dee-voltage of V_{DeeMax} corresponds to a pickup-loop voltage that is frequency dependent. This frequency-dependence of the peak-detector RF-input level requires an additional scaling factor to be employed; the attenuator.

A block diagram representing the feedback scaling is shown below:

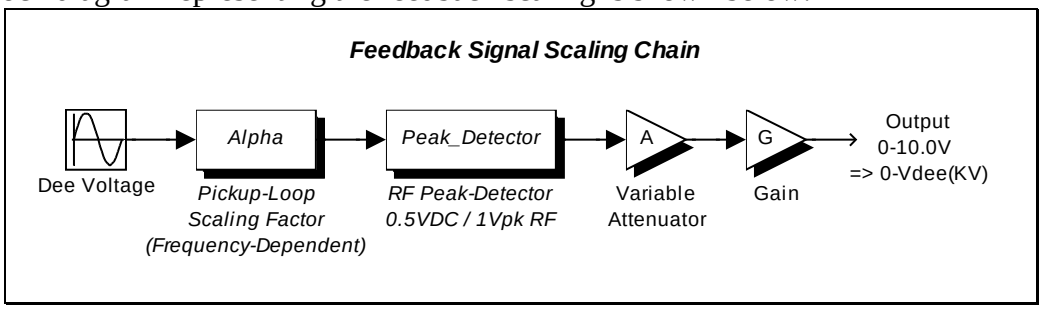

The variable attenuator is used to compensate for the frequency-dependence of the dee-voltage pickup-loops. Mathematically, the overall scaling is represented as

$$\boxed{Feedback\ Signal = V_{Dee} \cdot \alpha\ (f) \cdot 0.5 \cdot Atten(f) \cdot Gain}$$

where V_{Dee} is the dee-voltage in (KV_{pk}), $\alpha\,(f)$ is the pickup-loop scaling factor in (V/KV) (the inverse of the scaling factors given in *The RF Input Operating Range* section) , 0.5 is the peak-detector scaling factor, $Atten(f)$ is the attenuator scaling that is variable over 0-1, and $Gain$ is a predetermined gain which sets the low-frequency attenuator value close to unity (leaving some head-room for calibration).

The variable attenuator is a function of frequency in order to compensate for the pickup-loop scaling factor frequency-dependence. It is calculated based upon the fact that a 10.0V feedback-signal should correspond to the desired full-scale dee-voltage, $V_{Dee\ FS}$. The equation dictating the attenuator calculation is as follows:

$$\boxed{Atten(f) = \frac{10.0}{V_{Dee\ FS}} \cdot \frac{1}{0.5 \cdot Gain \cdot \alpha\,(f)}}\ .$$

The attenuator is realized using a 12-bit Multiplying Digital-to-Analog converter (MDAC). 12-bits were chosen in order to achieve a certain dee-voltage resolution per count even at the highest attenuation (or smallest digital word). The calculation was based upon the following:

1.) Assume the attenuator is equal to unity (1) at the lowest frequency. This will correspond to a digital value of 2^{x-1}, where *x* is the number of bits available on the MDAC.
2.) The attenuator will be at its lowest value (or maximum attenuation) at the highest frequency since the pickup-loop voltage goes up as a function of frequency. The attenuator value at the highest frequency (27MHz) is represented as $Atten(f_{\max})$. Its corresponding digital value, $D(f_{\max})$, will be $\frac{Atten(f_{\max})}{Atten(f_{\min})} \cdot 2^{x-1}$ which is just $Atten(f_{\max}) \cdot 2^{x-1}$ since it is assumed that $Atten(f_{\min}) = 1$.
3.) The resolution at maximum attenuation thus becomes $\frac{V_{Dee\ FS}}{D(f_{\max})}$ (Volts/count). As a percent of full-scale, this resolution is expressed as $\frac{1}{D(f_{\max})}$.

From the equation for the attenuator value, it is clearly seen that,

$$\frac{Atten(f_{\max})}{Atten(f_{\min})} = \frac{\alpha(f_{\min})}{\alpha(f_{\max})}.$$

Thus, the resolution (in percent of full-scale) at maximum attenuation becomes,

$$\%\ resolution(f_{\max}) = \frac{\alpha(f_{\max})}{\alpha(f_{\min})} \cdot \frac{1}{2^{x-1}}$$

This equation could be used to find the % resolution at any frequency by replacing $f_{\max}$ with the frequency of interest. In order to determine how many digital bits are needed, the above equation is simply solved for *x* using the ratio between the extremes of the pickup-loop scaling factors. (Note: $\alpha(f)$ is the inverse of the pickup-loop scaling factor given in *The RF Input Operating Range* section.) The equation for *x* is given as

$$x = \frac{\ln\left(\frac{100}{P\%} \cdot \frac{\alpha(f_{\max})}{\alpha(f_{\min})} + 1\right)}{\ln(2)},$$

where P% is the desired resolution in percent of full-scale.

Looking at the pickup-loop scaling factors in *The RF Input Operating Range* section (and remembering that those values are the inverse of α, the calculation of *x* is tabulated in the following table:

Cyclotron	f_{min} (MHz)	f_{max} (MHz)	$\alpha(f_{min})$ (V/KV)	$\alpha(f_{max})$ (V/KV)	Desired %Resolution (%)	MDAC bits
K500	11	27	0.035	0.148	0.1	12.06
K1200	9.5	27	0.016	0.089	0.1	12.45

Although, we would need 13 bits to satisfy 0.1% resolution per count at the highest frequency, 12-bits will suffice.

Note: The %resolution per count means that for a one count change in attenuation value the displayed dee-voltage will change by a value equal to that percent of the full-scale dee-voltage range.

Going back to the feedback-signal overall scaling, the selection of the *Gain* term was based upon the following:

1.) It is desired to have some headroom in the attenuator value at the lowest frequency. In otherwords, calculating the *Gain* term based upon an attenuator value of exactly unity at the lowest frequency does not allow any room if the attenuator value needs to be slightly increased during calibration. The chosen headroom is 50 counts below unity. Thus the lowest frequency attenuator value is 4045 out of 4095.

2.) A value slightly less than unity is selected for the attenuator at the lowest RF frequency. Using this less-than-unity value, a *Gain* is calculated that will result in a 10.0V signal at the maximum dee-voltage.

3.) Using this value for the *Gain* term, the attenuator values as a function of frequency are calculated for both cyclotrons using the pickup-loop scaling factors in conjunction with the additional pickup-loop scaling factor introduced by the peak-detector's frequency-dependence.

The expression for the *Gain* term based upon the 50 counts of headroom is as follows:

$$Gain = \frac{10.0}{V_{Dee\ FS}} \cdot \frac{1}{0.5 \cdot \alpha\,(f_{\min}) \cdot \left(\frac{4055}{4095}\right)} \ ,$$

where $\alpha\,(f_{\min})$ is the total pickup-loop scaling factor at the lowest frequency and $V_{Dee\ FS}$ is the full-scale dee-voltage ($100KV_{pk}$ for the K500 and $200KV_{pk}$ for the K1200). The calculation of the gain for both the K500 and the K1200 is tabulated below:

Calculated Feedback Scaling Gain

Cyclotron	Full-Scale Dee Voltage (KV_{pk})	f_{min} (MHz)	Pickup-Loop Factor (V_{Loop} / KV_{dee})	Additional Scaling from Peak-Detector	Required Feedback Gain
K500	100	11	0.0349	0.988	5.86
K1200	200	9.5	0.0159	0.982	6.46

The exact gain values above cannot be realized with standard resistor values. However, the nearest attainable value will be chosen based upon common resistor values. The gain is realized using a standard inverting op-amp whose gain is determined by the ratio of its feedback-resistor to its input-resistor. Both of these resistors can be easily changed on the motherboard through a component header which will be discussed later. For now, the gain-stage input-resistance and feedback-resistance values will be tabulated along with the achieved gain.

Feedback Gain Realized with Actual Resistors

Cyclotron	Desired Gain	Input-Resistance (kΩ)	Feedback-Resistance (kΩ)	Actual Gain
K500	5.86	2.52	15	5.95
K1200	6.46	2.67	17.4	6.52

It is the above gain that is actually used. Thus, this is the gain which will also used to determine the attenuator values as a function of frequency.

K500 DVR Attenuator Value Calculation with Feedback Gain = 5.95 and $V_{Dee\ FS}$ = 100KV_{pk}

Frequency (MHz)	Pickup-Loop Scaling Factor (V_{Loop} / KV_{Dee})	Additional Scaling from Peak-Detector	Total Pickup-Loop Scaling (V_{Loop} / KV_{Dee})	Calculated Attenuation Value	DVR Attenuator Setting (xx / 4095)
11	0.0349	0.988	0.0344	0.976	98
13	0.0457	0.997	0.0456	0.738	1074
15	0.0581	1.005	0.0584	0.576	1738
17	0.0715	1.013	0.0724	0.464	2194
19	0.0859	1.021	0.0877	0.383	2526
21	0.1010	1.030	0.1040	0.323	2772
23	0.1167	1.038	0.1211	0.278	2959
25	0.1325	1.046	0.1385	0.243	3101
26.5	0.1441	1.052	0.1516	0.222	3187
27	0.1484	1.054	0.1564	0.215	3215

K1200 DVR Attenuator Value Calculation with Feedback Gain = 6.52 and $V_{Dee\ FS}$ = 200KV_{pk}

Frequency (MHz)	Pickup-Loop Scaling Factor (V_{Loop} / KV_{Dee})	Additional Scaling from Peak-Detector	Total Pickup-Loop Scaling (V_{Loop} / KV_{Dee})	Calculated Attenuation Value	DVR Attenuator Setting (xx / 4095)
9.5	0.0159	0.982	0.0156	0.981	77
11	0.0198	0.988	0.0196	0.783	889
13	0.0259	0.997	0.0258	0.594	1664
15	0.0326	1.005	0.0328	0.468	2180
17	0.0396	1.013	0.0401	0.383	2528
19	0.0475	1.021	0.0485	0.317	2799
21	0.0555	1.030	0.0571	0.268	2996
23	0.0652	1.038	0.0677	0.227	3167
25	0.0794	1.046	0.0831	0.185	3339
26.5	0.0871	1.052	0.0916	0.167	3410
27	0.0893	1.054	0.0941	0.163	3428

Note: The DVR attenuator setting is an attenuation value, thus 0=no attenuation while 4095=max attenuation. The last column is calculated as (1-AttenuationValue)*4095.

The RF Amplitude Controller

The RF Amplitude Controller is the actuator for the voltage regulation system. Its design was based upon the Analog-Devices AD835, an 250MHz analog multiplying chip. The amplitude-controller is designed to accept a 0-10V command signal and output a 0-V_{RF} signal, where V_{RF} is a settable full-scale RF voltage level. The board does not have a RF generator, rather it multiplies an RF-input to generate the variable output. Furthermore, the full-scale RF output level remains fixed for a certain range of RF-input levels; thereby eliminating any output fluctuations due to input fluctuations.

The block diagram for the RF Amplitude-Controller is shown below:

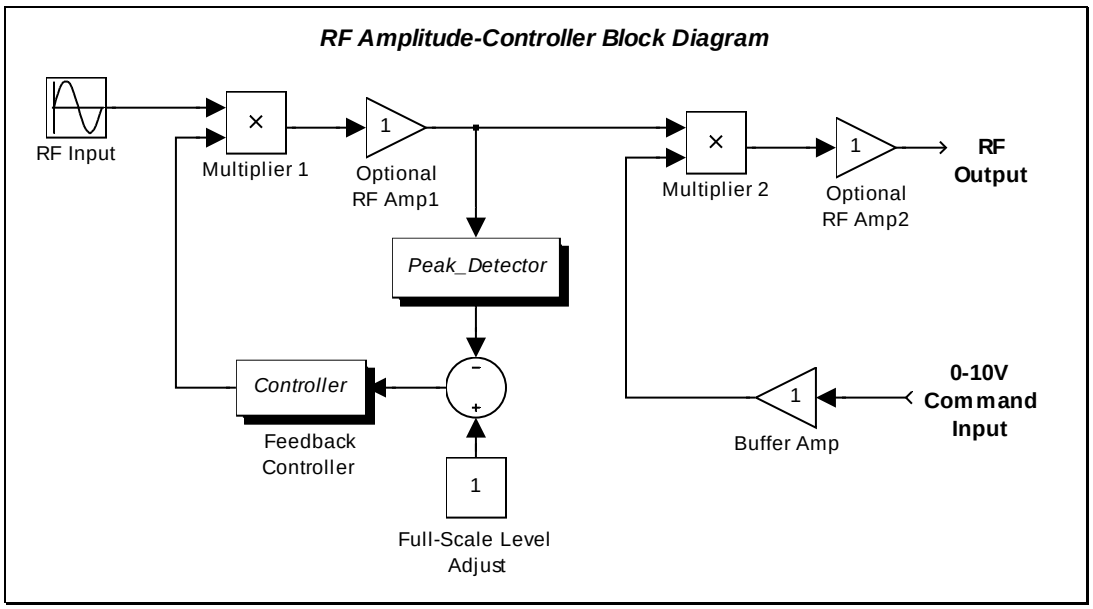

The first multiplier is used for making the output impervious to RF input fluctuations, while the second multiplier is used for achieving the response to the command input.

The detailed schematic for the RF amplitude-controller can be found in the documentation bundle for the DVR.

The RF Peak-Detector and RF Amplitude-Controller Dynamic Responses

In order to measure the dynamic response of both the RF Amplitude Controller and the RF Peak Detector, the experimental setup represented below was used.

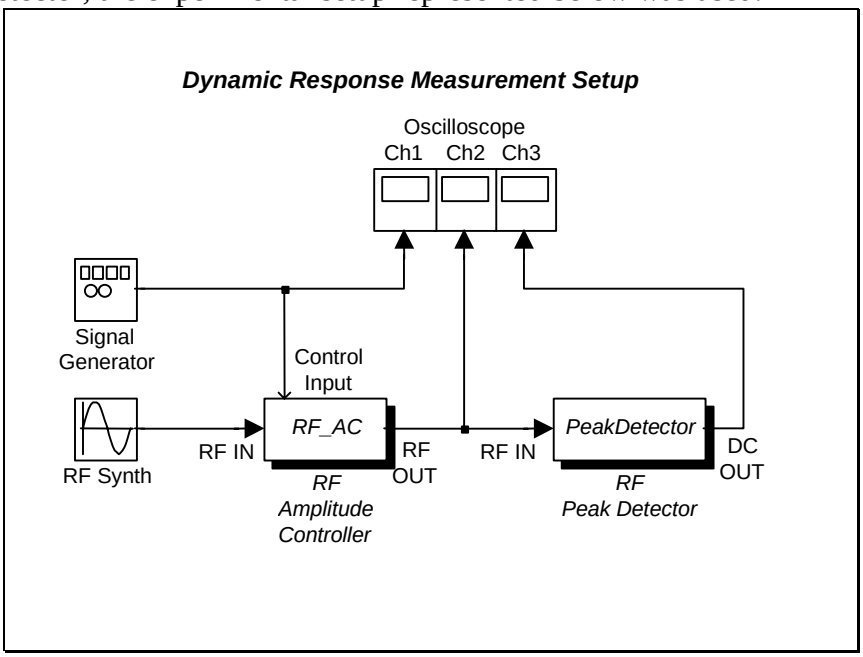

Experimental Dynamic Response Measurement

The signal generator, while being monitored at the oscilloscope, was used to feed a dc-offset, low-frequency, sinusoidal amplitude-control signal to the RF Amplitude Controller. The RF output of the RF Amplitude Controller was then fed into the RF Peak Detector while being monitored at the oscilloscope. By appropriately setting up the scope's triggering, the amplitude and phase (relative to the signal generator) of the resultant RF amplitude-modulation signal coming from the RF Amplitude Controller was measured. Finally, the amplitude and phase (relative to the signal generator) of the RF Peak Detector's DC output was also measured at the oscilloscope.

Thus, the amplitude and phase measurements of the RF Amplitude Controller at scope-channel 2 was a direct measurement of the dynamic response of the Amplitude Controller. On the other hand, the amplitude and phase measurements at the Peak Detector's DC output were a dynamic response measurement of both the Amplitude Controller and the Peak Detector. However, the Peak Detector's isolated response was determined by extracting out the Amplitude Controller's response from the combined response. The theoretical justification of this procedure was already discussed in RF Note 118, 'RF Control System Characterization'.

The experimental data for the isolated dynamic response of the Amplitude Controller and the combined response of the Amplitude Controller and Peak Detector can be found in the proceeding figures.

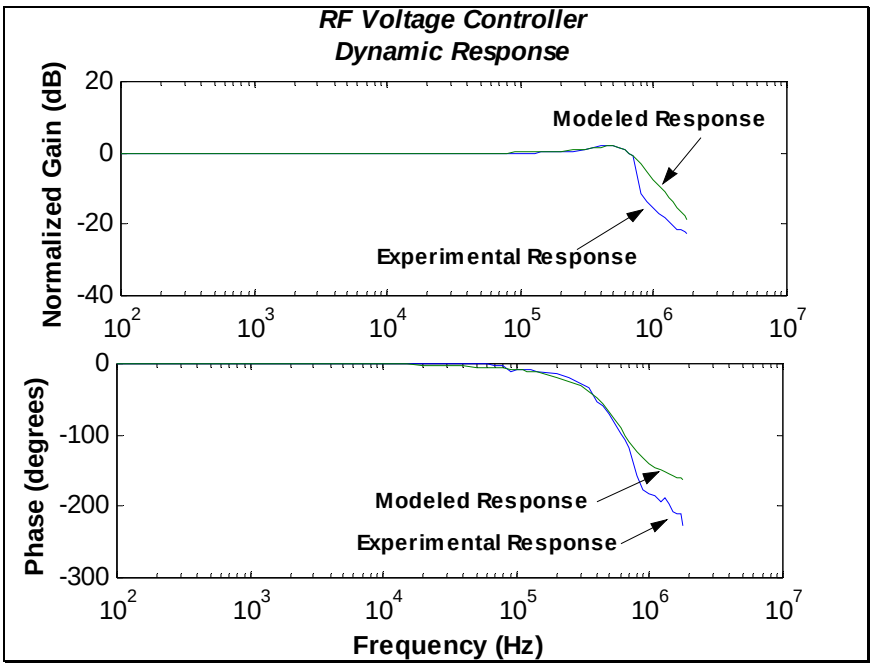
RF Voltage Controller
Dynamic Response
Normalized Gain (dB)
20
0
-20
-40
Modeled Response
Experimental Response
10^2
10^3
10^4
10^5
10^6
10^7
Phase (degrees)
0
-100
-200
-300
Modeled Response
Experimental Response
Frequency (Hz)

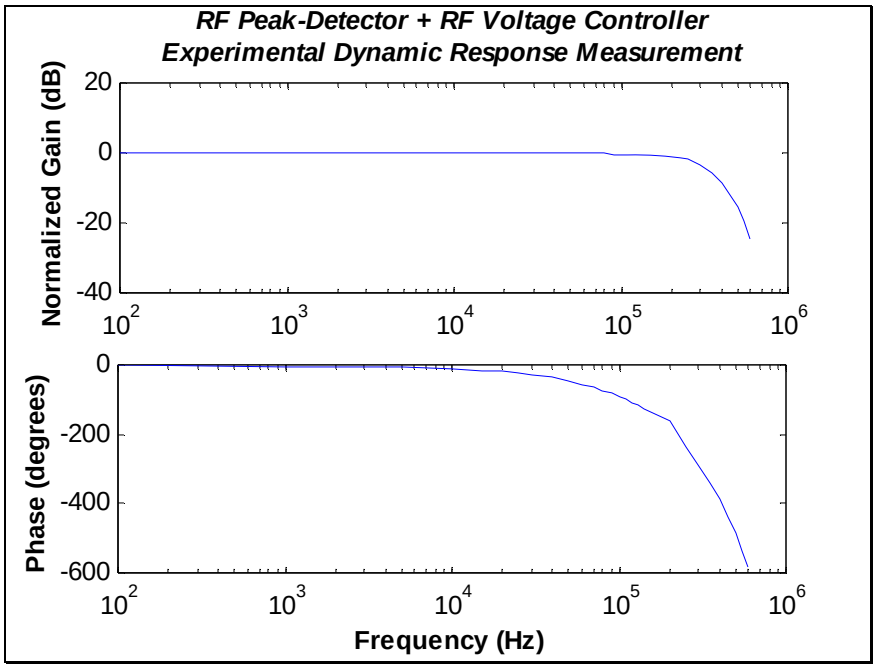
RF Peak-Detector + RF Voltage Controller
Experimental Dynamic Response Measurement
Normalized Gain (dB)
20
0
-20
-40
10^2
10^3
10^4
10^5
10^6
Phase (degrees)
0
-200
-400
-600
Frequency (Hz)

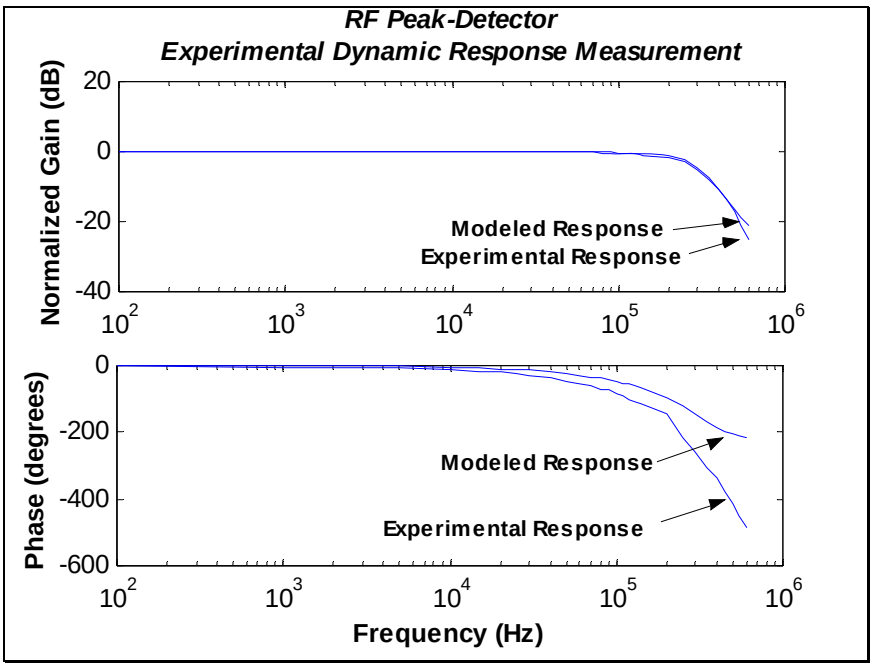

The models used for the RF Amplitude-Controller and the RF Peak-Detector are given below.

$$RF\ \ AmpCont(s) = \frac{(\omega_{amp})^2}{s^2 + 2 \cdot \zeta_{amp} \cdot \omega_{amp} \cdot s + (\omega_{amp})^2}$$

where $\omega_{amp} = 2\pi \cdot 600 \cdot 10^3$ and $\zeta_{amp} = 0.45$

$$RF\ \ PeakDet(s) = \frac{\omega_{Det1} \cdot (\omega_{Det2})^2}{(s + \omega_{Det1}) \cdot (s^2 + 2 \cdot \zeta_{Det} \cdot \omega_{Det2} \cdot s + (\omega_{Det2})^2)}$$

where $\omega_{Det1} = 2\pi \cdot 200 \cdot 10^3$, $\omega_{Det2} = 2\pi \cdot 300 \cdot 10^3$, and $\zeta_{Det} = 0.5$

The models are only approximate fits to the experimental data. They can be used for an initial closed-loop design based upon the root-locus design technique. However, when determining the actual closed-loop response and disturbance-rejection, the experimental bode plots should be used.

The Closed-Loop Design

The design of a closed-loop control system is embarked upon by investigating the system's open-loop behavior. It is from this investigation that the final feedback compensation design is derived. In particular, the voltage-regulation loop is a classical single-input/single-output (SISO) linear system; a type of control system whose analysis has been developed into a well-documented science over the past century. Thus, the design method presented here is nothing new. Merely, it is the particulars of the design and its impact on the characteristics of the voltage-regulation system which is of interest.

A block diagram of the closed-loop voltage regulation system is shown below:

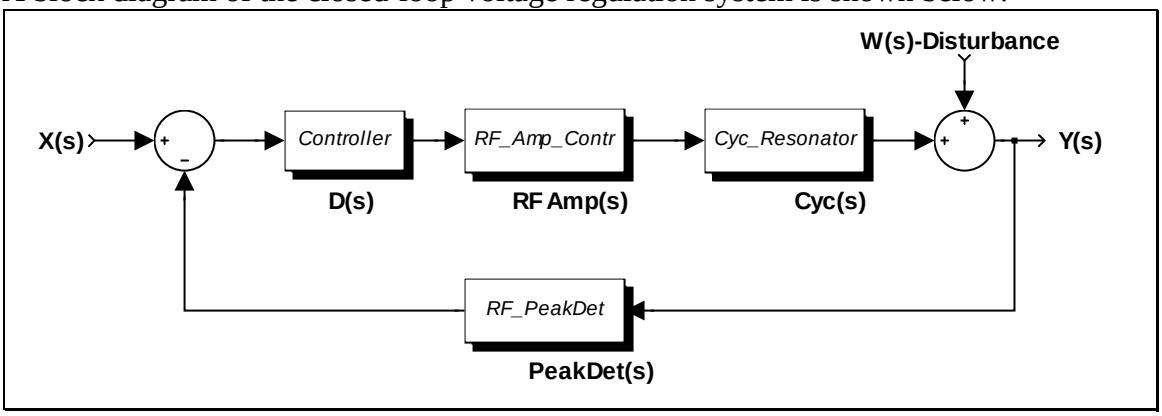

Closed-Loop System Block Diagram

where *X(s)* is the LaPlace transform of the input function, *D(s)* is the LaPlace transfer function of the closed-loop dynamic compensator, *RFAmp(s)* is the transfer function of the RF Amplitude-Controller, *Cyc(s)* is the transfer function of the cyclotron dee-resonator, *PeakDet(s)* is the transfer function of the RF Peak-Detector, and *Y(s)* is the LaPlace transform of the output function, and *W(s)* is the LaPlace transform of the disturbance function.

The closed-loop transfer function is represented as,

$$\frac{Y(s)}{X(s)} = \frac{D(s)\cdot RFAmp(s)\cdot Cyc(s)}{1 + D(s)\cdot RFAmp(s)\cdot Cyc(s)\cdot PeakDet(s)}$$

The stability of this system is determined by its pole locations, which happen to be the roots of the transfer function's denominator. The equation to determine the denominator roots has been termed the 'characteristic equation' and is given as:

$$1 + D(s)\cdot RFAmp(s)\cdot Cyc(s)\cdot PeakDet(s) = 0 \ .$$

Since all components except for *D(s)* are fixed, *D(s)* is designed to position the closed-loop pole locations for a certain degree of stability.

Furthermore, *D(s)* is also designed for noise-disturbance rejection. From the same closed-loop block diagram, the transfer function from disturbance *W(s)* to output *Y(s)*, is given as,

$$\frac{Y(s)}{W(s)} = \frac{1}{1 + D(s) \cdot RFAmp(s) \cdot Cyc(s) \cdot PeakDet(s)}$$

which has the same poles as the input-to-output transfer function, but different zeros.

The particular form of *D(s)* consists of a proportional and integral term. The integral term is approximated by using a lag-compensator. A derivative term was not used since the design did not require dynamic tracking of the input, but rather only steady-state regulation about the input. The mathematical form for *D(s)* is given as

$$D(s) = K_P + K_I \cdot \frac{(s+z)}{(s+p)}$$

where K_P is the proportional gain, K_I is the lag-compensator gain, z is the lag-compensator zero, and p is the lag-compensator pole. The proportional term is used to give more flexibility in designing the closed-loop system pole-locations. The lag-compensator increases the open-loop DC gain, thereby decreasing the steady-state error, while minimally affecting the stability (due to the zero eventually nulling out the pole).

Before presenting the final design for *D(s)* it is interesting to discuss the factors which influenced its design.

The Influence of the Resonator Dynamic Response

As discussed in the *Cyclotron Dynamic Response Characterization* section, the resonator pole/zero model changes as a function of frequency. In particular, as the Q decreases as a function of frequency, the complex conjugate poles and zero move increasingly to the left in the s-plane; indicating an increasing bandwidth.

The restriction that the resonator dynamic response places upon the closed-loop compensator, *D(s)*, is a restriction on the placement of the lag-compensator zero. When designing the pole/zero locations for a lag-compensator, the pole is chosen very close to the origin. The lag-compensator zero is placed far to the left of the pole in order to maintain a high DC gain. However, the location of the zero should not interfere with the dynamics of the uncompensated system. This means that the zero location should be placed to the right of the smallest pole (or zero) location of the uncompensated open-loop system. Since the cyclotron resonator is the lowest bandwidth device within the uncompensated voltage-regulation system, its pole/zero locations place the restriction on the lag-compensator zero-position.

In particular, the resonator's lowest bandwidth occurs at the lowest frequency (highest Q). Thus, the lag-compensator zero must be placed to the right of the resonator's poles/zero at the lowest operating frequency (9.5MHz for the K1200, 11MHz for the K500).

In order to understand the second effect that the resonator dynamic response has on the compensator design, a simple proportional-term compensator design will be used. This allows for a simple Root Locus Design technique to be applied. For this case, *D(s)*, simply becomes K_P and the characteristic equation is simply,

$$1 + K_P \cdot RFAmp(s) \cdot Cyc(s) \cdot PeakDet(s) = 0$$

The root-locus is a plot of the closed-loop pole locations as a function of increasing proportional-gain, K_P.

The root-locus for the voltage-regulation system with a simple proportional-gain term is plotted below for the K1200 at the two operating RF frequency extremes, 9.5MHz and 26.5MHz.

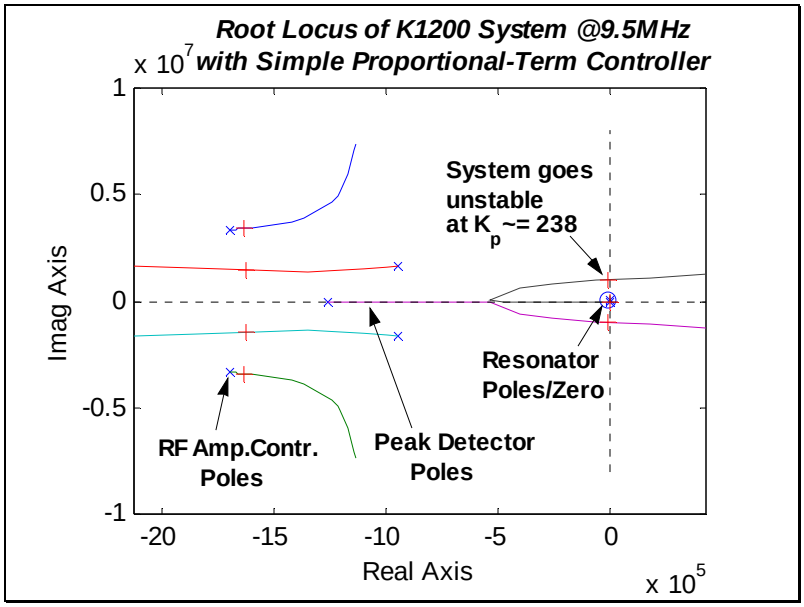

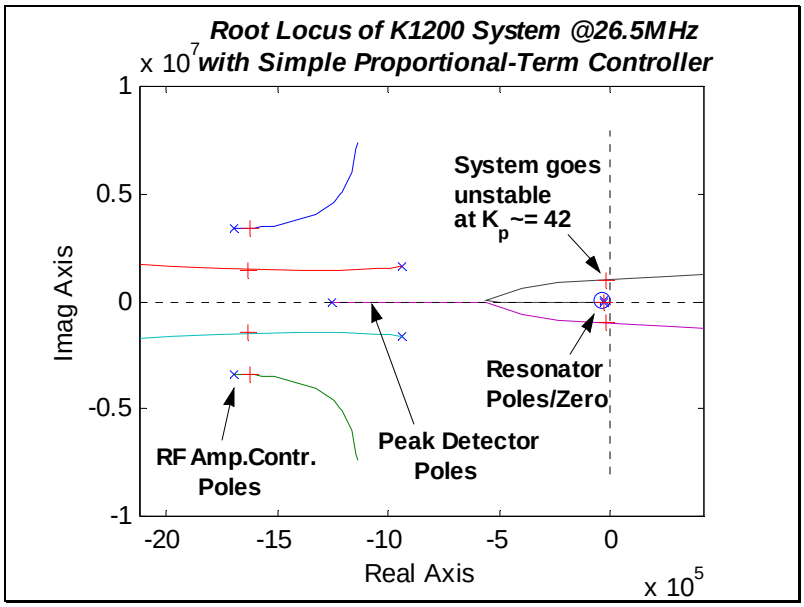

From the above two plots, it is seen that the closed-loop system goes unstable at a lower proportional-gain at 26.5MHz than at 9.5MHz. This is due to the lower initial phase-margin at 26.5MHz as compared to 9.5MHz. The phase-margin is better viewed from the bode-plot of the open-loop system. The bode plots for the open-loop voltage-regulation system at 9.5MHz and 26.5MHz are shown below:

Note: The decrease in allowable proportional gain as the operating frequency is increased is conveniently accounted for by the inherent decrease in the transmitter/resonator open-loop gain as discussed previously. More details will follow.

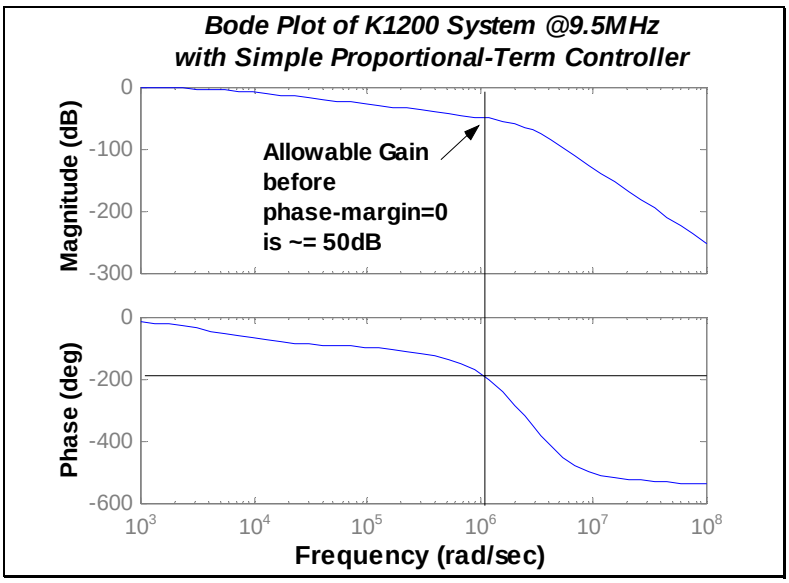

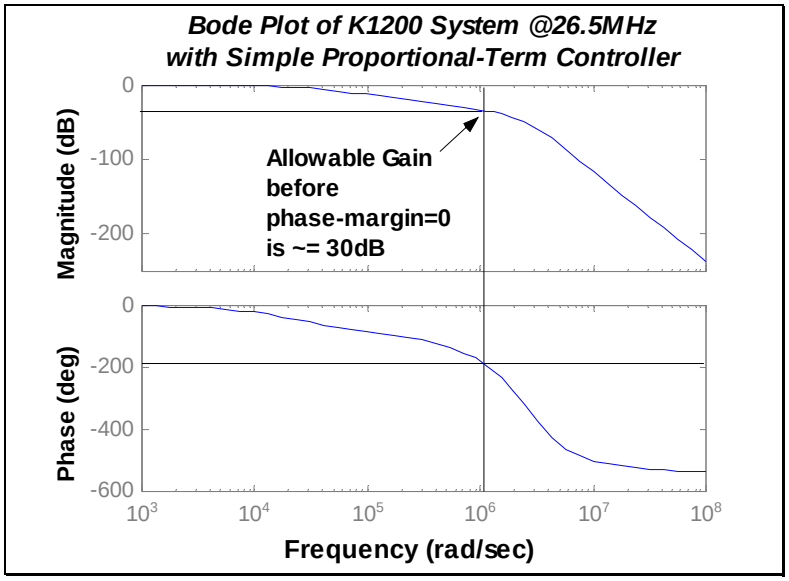

The above bode plots are a different way by which to view the design. They do indeed correlate to the root locus predictions of a lower allowable proportional-gain at 26.5MHz than at 9.5MHz.

The stability of a proportional-term controller improves as the frequency is lowered. However, from a similar analysis, the stability of a lag-network controller worsens as the frequency is lowered.

System Time-Delay

Before presenting the experimental results, it is important to note that the theoretically predicted step-response did not initially correlate well with the experimental measurements. The initial problem with the theoretical model was that it did not include the time-delay of the system. The time-delay in the system is a result of the pickup-loop cables and the time-delay through the RF transmitters. In particular, the time-delay between the DVR RF output and the transmitter's Driver Anode probe was measured to be approximately 2μs while the delay between the Driver Anode and the RF balcony dee-voltage pickup-loop was measured to be approximately another 0.5μs. Thus the total time-delay in the open-loop system is approximately 2.5μs. This time delay was then included in the theoretical model which was used in the data that is to be presented below.

The time-delay was measured by applying a square wave modulation signal to the DVR and measuring the delay between the start of the square-wave on the RF output of the DVR and the start of the square-wave on the dee-voltage pickup-loop signal.

The system time-delay is summarized below for convenience.

Time-Delay from DVR RF Output and Transmitter Driver Anode: ~2μs

Time-Delay from Transmitter Driver Anode and RF Balcony Pickup-Loop: ~0.5μs

Total System Time Delay: ~2.5μs

Experimental Investigations on the K1200 Closed-Loop System

The theoretical dynamic response model for the entire open-loop system is the basis for an initial closed-loop design as well as for qualitative analyses. However, the final design needs to function on the actual physical system. Therefore, experimental investigations need to confirm the performance of the closed-loop system. These experimental investigations can also be used to correlate the theoretical model to the actual system; hopefully giving confidence that the theoretical model can be used for mathematical calculations, etc.

Initial experimental investigations on the K1200 consisted of biasing the dee-voltage to different levels and applying a square wave command signal to the DVR in closed-loop, thereby measuring the step-response of the voltage-regulation system at different open-loop gains. The different open-loop gains arise from operating at different bias dee-voltages. (From the discussion of the transmitter/resonator open-loop gain, it was shown that the open-loop gain is a function of dee-voltage).

Since the dee-voltage cannot be measured without the RF peak-detector, the RF peak-detector had to be considered part of the open-loop system with its output representing the system output. This system is shown below:

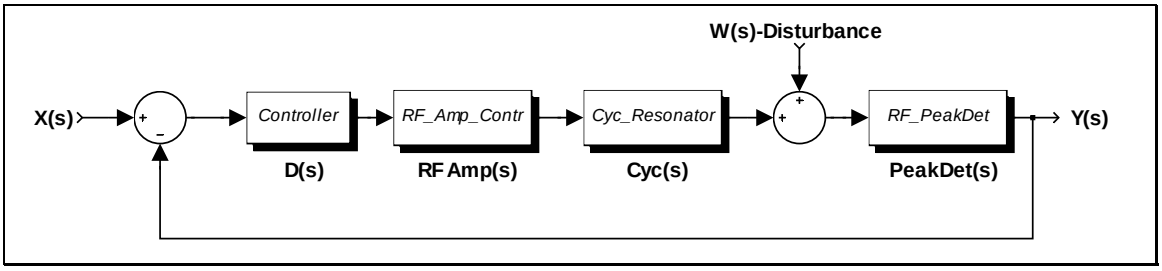

Experimental Closed-Loop System Block Diagram

The dynamic compensation used in the closed-loop controller consisted of a proportional term and a lag-compensator. The proportional-gain and the lag-compensator gain were varied independently during the measurements in order to obtain step responses for different controller dynamics. This allowed for a better correlation between the actual system and the theoretical model.

The lag-compensator pole and zero locations, however, were fixed during these measurements. In particular, the complete expression for *D(s)* took the form of

$$D(s)_{Exper} = K_p + K_I \cdot \frac{(s + 2\pi \cdot 300)}{(s + 2\pi \cdot 1)}$$

where K_P and K_I were varied. The values used for K_P and K_I are noted in the experimental data.

Experimental Closed-Loop Measurements at 18.3MHz

The experimental closed-loop step response at an RF operating frequency of 18.3MHz was measured at dee-voltage of $25KV_{pk}$, $60KV_{pk}$, and $100KV_{pk}$. Based upon the full-scale DVR RF output level and the open-loop gain of the transmitter/resonator system, the equivalent open-loop gain of the system at these levels were 0.67, 0.94, and 1.19 respectively.

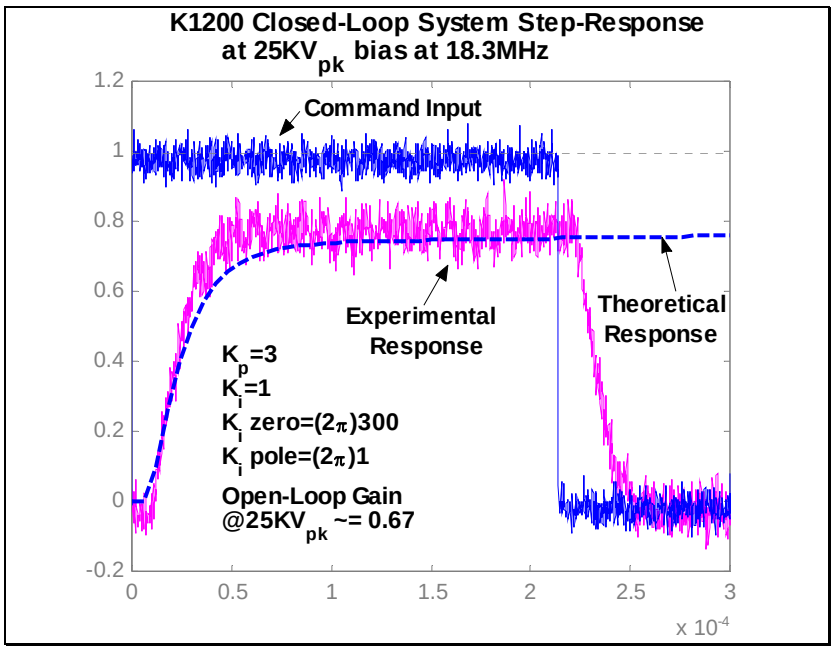

Closed-Loop Response for 18.3MHz at $25KV_{pk}$ (open-loop gain~=0.67)

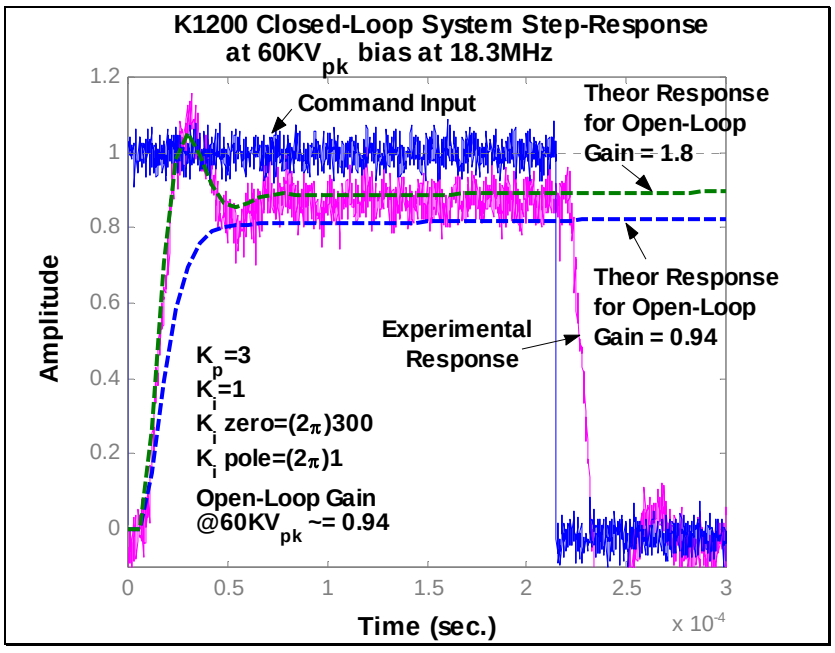

Closed-Loop Response for 18.3MHz at $60KV_{pk}$ (open-loop gain~=0.94)

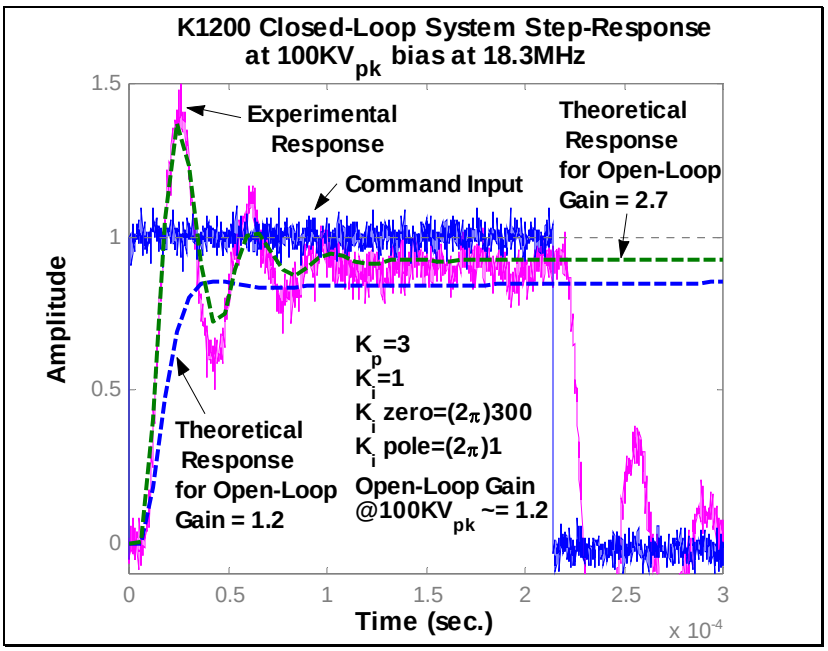

Closed-Loop Response for 18.3MHz at 100KV$_{pk}$ (open-loop gain~=1.2)

From the above three graphs, it is evident that the theoretical model predicts less overshoot and oscillations than the actual physical system. The theoretical open-loop gain which corrects for this is displayed in the graphs as the theoretical response that better correlates with the experimental results. The reason why the theoretical model does not predict the correct overshoot is due to the models of the RF Amplitude-Controller and the RF Peak-Detector. Looking back at those models, the phase response of the theoretical model under-estimates the phase response of the actual data. Thus, the phase-margin of the theoretical system will appear greater than the phase-margin of the actual system.

To correlate the theoretical model with the physical system, an additional time-delay factor of 2μs was added as well a factor of approximately 2 was added to the open-loop gain. Thus the discrepancy between the theoretical model and the physical system was compensated for by distributing the differences with a time-delay (phase lag) and an additional open-loop gain. From the above graphs, adding these factors more closely correlates the theoretical model to the physical system.

Noise Rejection Investigations

The most important specification of the dee-voltage regulation system is how well it can regulate the dee-voltage in the presence noise. This noise enters the system through various channels such as mechanical vibrations, thermal heating, transmitter bias power-supply fluctuations, line-noise in the electronics modules, etc. Due to the dynamic response of the dee-resonator, the bandwidth of the dee-voltage noise is restricted to approximately 4.5 KHz. (Note: This is the highest bandwidth of the resonator occuring at 27MHz for both cyclotrons). Thus all of the noise measurements presented here were low-pass filtered at 10 KHz. In fact, open-loop noise measurements indicated that no noise above 2KHz existed inside the dee-resonator.

Note: All noise measurements were 10KHz low-pass filtered. Note also that the FFT spectrum of a sample function of the noise is only used as a means of measuring the disturbance rejection ratio at a particular frequency. In order to use these noise sample functions properly, spectral density functions would have to be developed. If this was done, then a quantified value could be placed on the actual noise level. The data presented here is available for future investigations of this sort. For now, as was said, these measurements are being used to measure the disturbance rejection as a function of frequency and to correlate this to the theoretical disturbance rejection.

After presenting the noise rejection investigations, the design of the closed-loop dynamic compensator can be finalized to achieve a certain disturbance-rejection ratio.

Before making system noise measurements, a baseline noise measurement of the oscilloscope itself was taken. This is presented below:

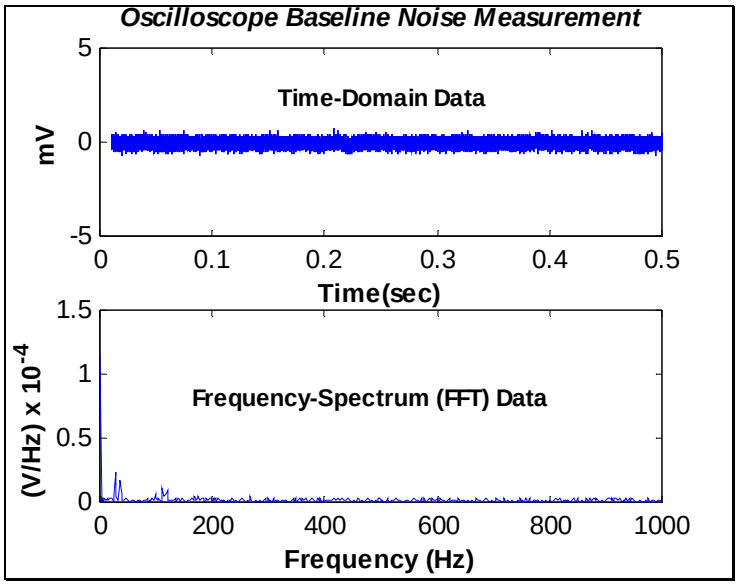

From the data, it is seen that the oscilloscope is capable of measuring with a resolution of 1mV. This is (1mV/10V)*100%=0.01% of our full-scale command.

Secondly, the noise of the peak-detector output was measured without any feedback scaling and with no RF on the dee-resonator. The data is given below:

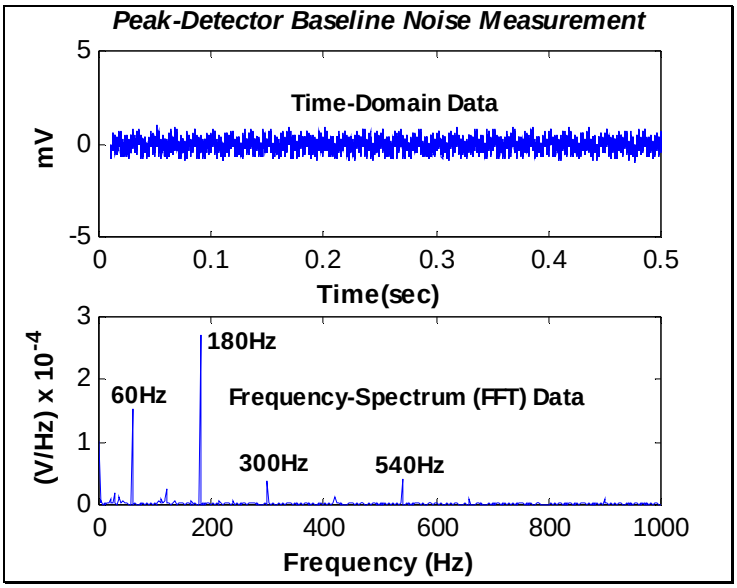

Note: This peak-detector noise is the noise which will be injected into the system since the peak-detector is telling the system that these noise components are in the system when in fact they are not. Furthermore, this is a stand-alone peak-detector without any feedback scaling.

The noise of the properly scaled feedback signal measured right on the DVR feedback op-amp is shown in the following plot. It is expected that this noise will be somewhat smaller than what is shown since the prototype did not have this op-amp routed on the PCB board, rather it consisted of some modified wiring that was coming off of the PCB board.

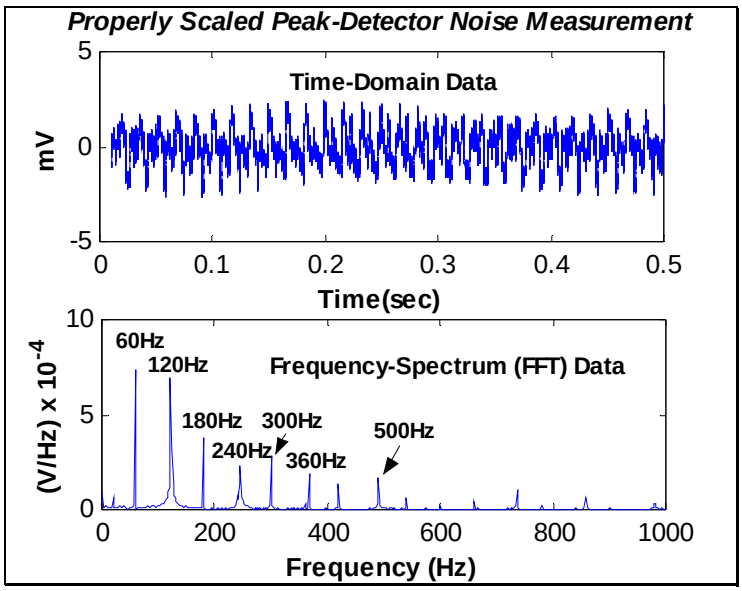

Again, the peak-detector noise will actually be injected into the system. It should not be subtracted out of the noise measurements that follow, rather it should be added to them. Only the oscilloscope baseline noise should be subtracted from the following data.

The Open-Loop Noise

The open-loop noise of the voltage-regulation system gives a measure of the noise that is in the system without any closed-loop regulation. It is the closed-loop controller that is suppose to eliminate this open-loop noise. The data presented here is used to determine the frequency spectrum of the open-loop noise. The closed-loop system must therefore attenuate this noise by a certain degree in order to maintain a specific regulation. Before giving any quantitative measures on the noise-rejection ratios the data will be presented.

The dominant component of the noise spectrum was found to be at 360Hz. The source of this noise is the transmitter anode bias-supply which is a 3-phase rectified supply. Naturally, the level of the 360Hz noise component is a function of the load on the supply (the amount of current required to drive the RF transmitters) Thus, it is a function of the dee-voltage level.

To obtain a measure of how the noise component varies as a function of drive level, the open-loop noise was measured for various dee-voltages at 26.5MHz. The highest dee-voltage for which the noise was measured was $135KV_{pk}$. This was the dee-voltage at which the screen of the final tube started to conduct (anode voltage swing reached E_{min}).

The open-loop noise data collected for the highest dee-voltage ($135KV_{pk}$) at 26.5MHz is presented below:

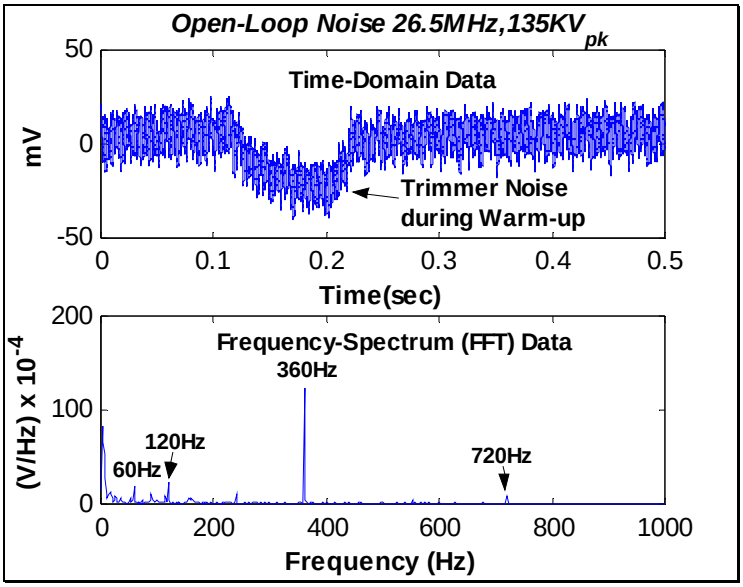

The peak-to-peak noise from the above data is seen to be approximately 30mV, excluding the trimmer noise. The trimmer noise is the sudden voltage fluctuation due to the dee-fine tuner trimmer moving during the initial dee-voltage turn-on.

A table of the FFT magnitude vs. dee-voltage at 26.5MHz for the main noise-components is given below. This table was generated from noise data similar to that shown above for a dee-voltage of 135KV_{pk}.

FFT Noise Data for 26.5MHz

	Frequency Component Noise (V/Hz x 10^{-4})				
Dee-Voltage (KV_{pk})	60Hz	120Hz	240Hz	360Hz	720Hz
20	5.3	12.0	3.9	21.9	1.6
40	8.9	12.8	5.1	30.4	1.8
60	13.8	13.8	5.4	33.5	2.8
100	18.4	17.4	6.9	46.6	3.2
125	13.1	15.5	7.2	70.6	4.9
135	19.6	23.3	10.3	123.2	8.1

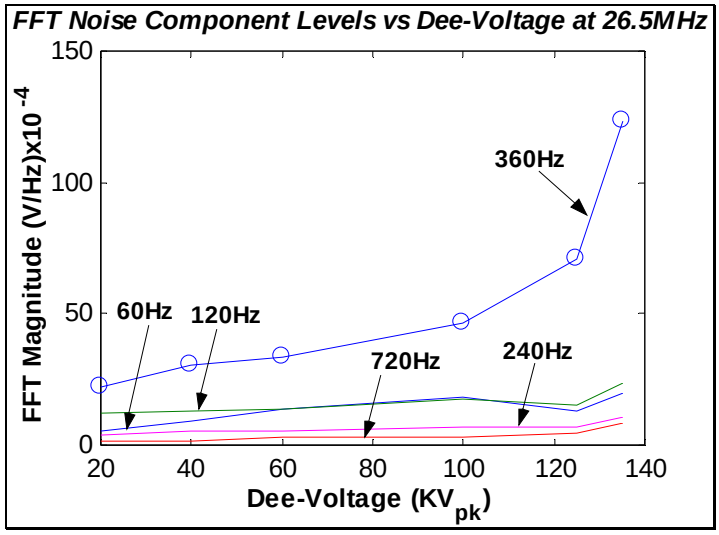

From the above plot, it is clearly evident that the main noise-component is at 360Hz and that this component is a strong function of the dee-voltage, indicating that it is due to the load presented to the final anode bias-supply. In particular, the last data point at 135KV_{pk} was the point at which the final screen began to conduct, indicating that the anode-voltage was swinging near to the tube's E_{min} value.

Note also that the lower frequency components are not influenced much by the dee-voltage.

Now, this open-loop noise, especially the 360Hz component needs to be reduced by the closed-loop regulation system. The above data is used as a reference to which to compare the closed-loop noise levels. From the open-loop noise and closed-loop noise, a measurement of the noise rejection ratio can be made for the above frequency components.

The Closed-Loop Noise

An experimental closed-loop noise measurement was made at 26.5MHz with a dee-voltage of $20KV_{pk}$. The dynamic compensation used for this measurement was a proportional gain of $K_P = 0.373$, a lag gain of $K_I = 6.79$ with the same lag-zero at $2\pi \cdot (300)$ radians/s and the same lag-pole at $2\pi \cdot (1)$ radians/s. The experimental data is shown below:

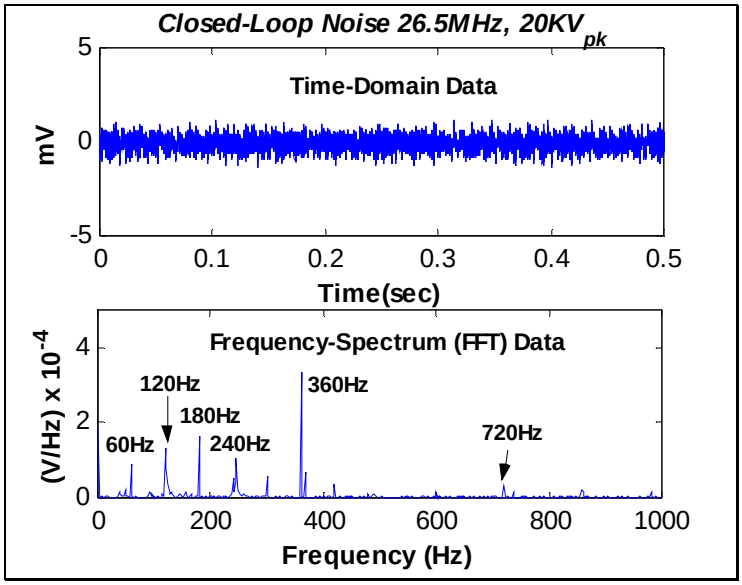

For comparison to the open-loop noise, the open-loop noise data for 26.5MHz at a dee-voltage of $20KV_{pk}$. is plotted below:

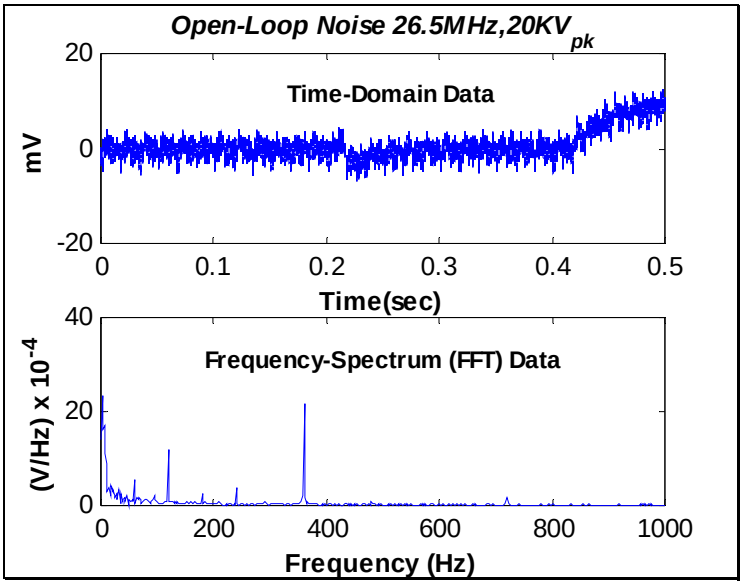

As seen in the data, this choice of dynamic compensation resulted in a closed-loop peak-to-peak noise measurement of approximately 2mV, the same level as the baseline noise measurement of the oscilloscope. Furthermore, the 360Hz open-loop noise level at $20KV_{pk}$ from the open-loop noise vs. dee-voltage graph is approximately $21.9x10^{-4}$ V/Hz. The closed-loop 360Hz noise level is only $3.34x10^{-4}$ V/Hz; implying a noise-rejection ratio of 3.34/21.9 = 0.1525 which is equivalent to –16.3dB.

The theoretical magnitude response from noise-disturbance to output for the experimental system is determined from the closed-loop block diagram repeated here:

Experimental Closed-Loop System

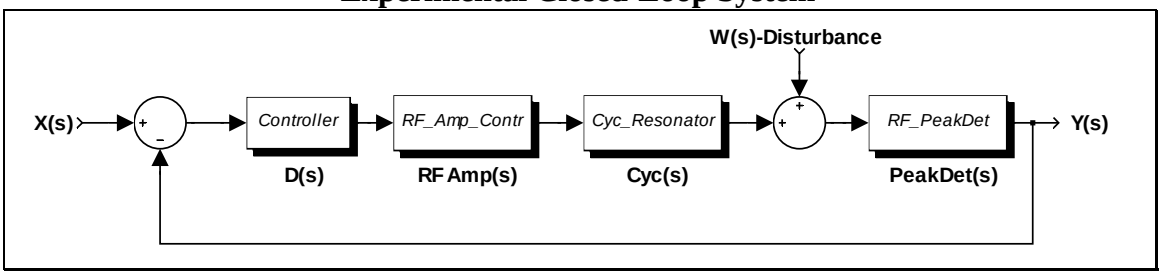

The transfer function is expressed as:

$$\frac{Y(s)}{W(s)} = \frac{PeakDet(s)}{1 + D(s) \cdot RFAmp(s) \cdot Cyc(s) \cdot PeakDet(s)}$$

The theoretical magnitude response (with the adjustment to the theoretical model of adding a factor of 2 to the open-loop gain and a 2us delay) is plotted below:

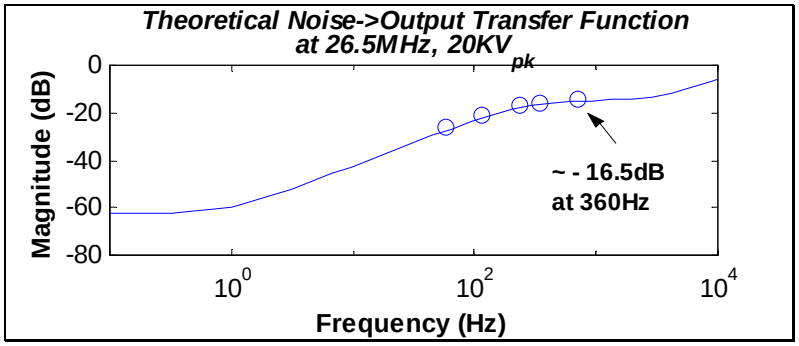

From the data, the theoretical noise rejection at 360Hz is –16.5dB, quite close to the measured value of –16.3 dB.

In order to achieve the same level of 360Hz noise at $135KV_{pk}$ as was achieved in closed-loop for $20KV_{pk}$, a disturbance rejection of 3.34/123.1 ~= -31dB. The final design goal will be to achieve –30dB of rejection at 360Hz.

The Design Guidelines

From all of the information presented in this note, the final closed-loop system is designed by the following guidelines.

1.) The closed-loop system should be made stable at all RF frequencies, taking into account the change in open-loop gain and the change in the resonator dynamics.
2.) In order to prevent any problems during initial turn-on of the system, the system should be either critically damped or over-damped so as to prevent any overshoot and oscillations.
3.) The disturbance rejection should be optimized such that the magnitude response of noise-to-output is the minimum value achievable at 360Hz. In particular, -30dB of rejection at 360Hz is desired.

Design guidelines 1 and 3 are contradictory guidelines, therefore a compromise has to be made between the two. The contradiction stems from an observation of the closed-loop transfer functions. Over-damping the closed-loop system implies a low feedback gain, while optimal disturbance rejection implies high feedback gain.

If a simpler proportional-term controller is used, the stability of the closed-loop system is worst case at 26.5MHz. However, if only a lag-network controller is used, the stability is worst case at the lowest frequency.

The lag-network is the ideal design candidate when considering disturbance rejection. The trade-offs for using pure lag-compensation is that the disturbance rejection and stability is best case at the highest frequency, while both disturbance rejection and stability worsen at lower frequencies. This is due to the resonator bandwidth decreasing for lower RF frequencies. Looking at the disturbance rejection transfer function, optimizing the disturbance rejection means maximizing the magnitude of the denominator for a given noise-frequency. This denominator, however, includes the resonator response whose magnitude decreases as the RF frequency is lowered.

The combination of a proportional plus a lag-network controller helps to balance the trade-offs of both stability and disturbance rejection. The reason for this is that the roots of the characteristic equation can be better manipulated by the combination of the two compensators.

Another factor which helps all of these tradeoffs is that the power-levels also decrease as the RF frequency is lowered. This means that there is less of a load on the anode bias-supply, thereby also implying that the 360Hz noise-component will also decrease as the RF frequency is lowered.

The K1200 Closed-Loop Design

The design goal was to achieve –30dB of rejection for 360Hz noise while maintaining up to a 30% overshoot across the RF frequency range. To achieve this goal, the overshoot and the 360Hz disturbance rejection was tabulated as the proportional-gain and the lag-gain was varied for a specified lag-zero and lag-pole. The lag-pole is fixed at $2\pi*(1)$. This achieves a certain steady-state error. The lag-zero was chosen in order to get the 360Hz noise-rejection within the desired range. The specific lag-zero chosen was $2\pi*(10000)$.

K1200
Overshoot at 26.5MHz in %
versus K_p and K_I
(note negative values indicate over-damping)

	K_P	0	0.1	0.2	0.3	0.4	0.5	0.6	0.7
KI									
0.1		10	1	-10	-10	-11	-15	-9	-2
0.2		19.5	10	5	0	-2	1	7	11
0.3		27.5	18	13	10.5	12	15	19	19
0.4		30	25	22	22	24	27	32	37
0.5		36	32	30	30	35	40	44	48
0.6		43	41	42	43	47	51	54	60
0.7		51	50	51	54	58	61	66	72
0.8		59	59	62	65	68	72	78	84

K1200
360Hz Noise-Rejection at 26.5MHz in -dB
versus K_p and K_I
(note values are negative indicating greater means better)

	K_P	0	0.1	0.2	0.3	0.4	0.5	0.6	0.7
KI									
0.1		18.1	18.1	18.2	18.3	18.4	18.5	18.6	18.7
0.2		24.1	24.1	24.1	24.2	24.2	24.2	24.2	24.3
0.3		27.6	27.6	27.6	27.6	27.7	27.7	27.7	27.7
0.4		30.1	30.1	30.1	30.1	30.1	30.2	30.2	30.2
0.5		32.1	32.1	32.1	32.1	32.1	32.1	32.1	32.1
0.6		33.6	33.6	33.7	33.7	33.7	33.7	33.7	33.7
0.7		35	35	35	35	35	35	35	35
0.8		36.1	36.1	36.2	36.2	36.2	36.2	36.2	36.2

K1200
Overshoot at 9.5MHz in %
versus K_p and K_I
(note negative values indicate over-damping)

	K_P	0	0.1	0.2	0.3	0.4	0.5	0.6	0.7
KI									
0.1		47.5	36	27	20	16	11	8	6
0.2		55	45	38	31	27	23	20	16
0.3		59	50	44	38	34	30	26	26
0.4		61	55	47	42	37	34	31	28
0.5		62	55	50	45	40	37.5	33	31
0.6		62	56	50.5	45	43	40	37	35
0.7		60	56	53	49	46	43	39	36
0.8		63	59	55	51	47	43	39	38

K1200
360Hz Noise-Rejection at 9.5MHz in -dB
versus K_p and K_I
(note values are negative indicating greater means better)

	K_P	0	0.1	0.2	0.3	0.4	0.5	0.6	0.7
KI									
0.1		21.5	21.5	21.5	21.6	21.7	21.8	21.9	22
0.2		27.6	27.6	27.7	27.7	27.7	27.7	27.7	27.8
0.3		31.2	31.2	31.2	31.2	31.2	31.2	31.3	31.3
0.4		33.7	33.7	33.7	33.7	33.7	33.7	33.8	33.8
0.5		35.7	35.7	35.7	35.7	35.7	35.7	35.7	35.7
0.6		37.3	37.3	37.3	37.3	37.3	37.3	37.3	37.3
0.7		38.6	38.6	38.6	38.6	38.6	38.6	38.6	38.6
0.8		39.8	39.8	39.8	39.8	39.8	39.8	39.8	39.8

Based upon the above tables, a proportional gain of 0.4 and an integral-gain of 0.5 was chosen for the final design. This corresponds to overshoot values of 35% at 26.5MHz and 40% at 9.5MHz. The disturbance rejection ratios are –32.1dB at 26.5MHz and –35.7dB at 9.5MHz.

The K500 Closed-Loop Design

The same tables of overshoot and disturbance-rejection were generated for the theoretical K500 system at its frequency extremes (26.5MHz and 11MHz). The results are given below:

K500
Overshoot at 26.5MHz in %
versus K_p and K_I
(note negative values indicate over-damping)

	K_P	0	0.1	0.2	0.3	0.4	0.5	0.6	0.7
KI									
0.1		8	1	-9	-9	-10	-14	-8	-2
0.2		18	10	4	-1	-2	2	6	13
0.3		24	17	12	11	11	16	21	26
0.4		30	25	22	22	24	28	33	37
0.5		36	33	32	33	36	41	45	50
0.6		43	42	42	43	48	52	55	62
0.7		51	51	51	56	59	62	68	74
0.8		60	59	63	66	69	74	80	86

K500
360Hz Noise-Rejection at 26.5MHz in -dB
versus K_p and K_I
(note values are negative indicating greater means better)

	K_P	0	0.1	0.2	0.3	0.4	0.5	0.6	0.7
KI									
0.1		18.1	18.1	18.2	18.3	18.4	18.5	18.6	18.7
0.2		24.1	24.1	24.1	24.2	24.2	24.2	24.2	24.3
0.3		27.6	27.6	27.6	27.7	27.7	27.7	27.7	27.7
0.4		30.1	30.1	30.1	30.1	30.2	30.2	30.2	30.2
0.5		32.1	32.1	32.1	32.1	32.1	32.1	32.1	32.1
0.6		33.6	33.7	33.7	33.7	33.7	33.7	33.7	33.7
0.7		35	35	35	35	35	35	35	35
0.8		36.1	36.2	36.2	36.2	36.2	36.2	36.2	36.2

K500
Overshoot at 11MHz in %
versus K_p and K_I
(note negative values indicate over-damping)

	K_P	0	0.1	0.2	0.3	0.4	0.5	0.6	0.7
KI									
0.1		35	23	15	9	5	30	1	-1
0.2		44	34	27	20	16	13	10	8
0.3		48	40	33	27	23	20	16	14
0.4		49	44	38	32	27	25	23	20
0.5		53	45	38	36	33	30	26	23
0.6		51	48	44	40	36	32	28	29
0.7		57	52	47	42	36	34	35	36
0.8		58	52	46	40	41	42	41	41

K500
360Hz Noise-Rejection at 11MHz in -dB
versus K_p and K_I
(note values are negative indicating greater means better)

	K_P	0	0.1	0.2	0.3	0.4	0.5	0.6	0.7
KI									
0.1		22.3	22.3	22.4	22.5	22.5	22.6	22.7	22.8
0.2		28.4	28.4	28.4	28.4	28.4	28.5	28.5	28.5
0.3		31.9	31.9	31.9	32	32	32	32	32
0.4		34.4	34.4	34.4	34.5	34.5	34.5	34.5	34.5
0.5		36.4	36.4	36.4	36.4	36.4	36.4	36.4	36.4
0.6		38	38	38	38	38	38	38	38
0.7		39.3	39.3	39.3	39.3	39.3	39.3	39.3	39.3
0.8		40.5	40.5	40.5	40.5	40.5	40.5	40.5	40.5

Based upon the above tables, a proportional gain of 0.4 and an integral-gain of 0.5 was chosen for the K500 final design. These are the same values as for the K1200. This corresponds to overshoot values of 36% at 26.5MHz and 33% at 11MHz. The disturbance rejection ratios are –32.1dB at 26.5MHz and –36.4dB at 11MHz.

The Controller Component-Values

The components which make up the proportional and integral (lag-compensator) terms are shown in the following picture

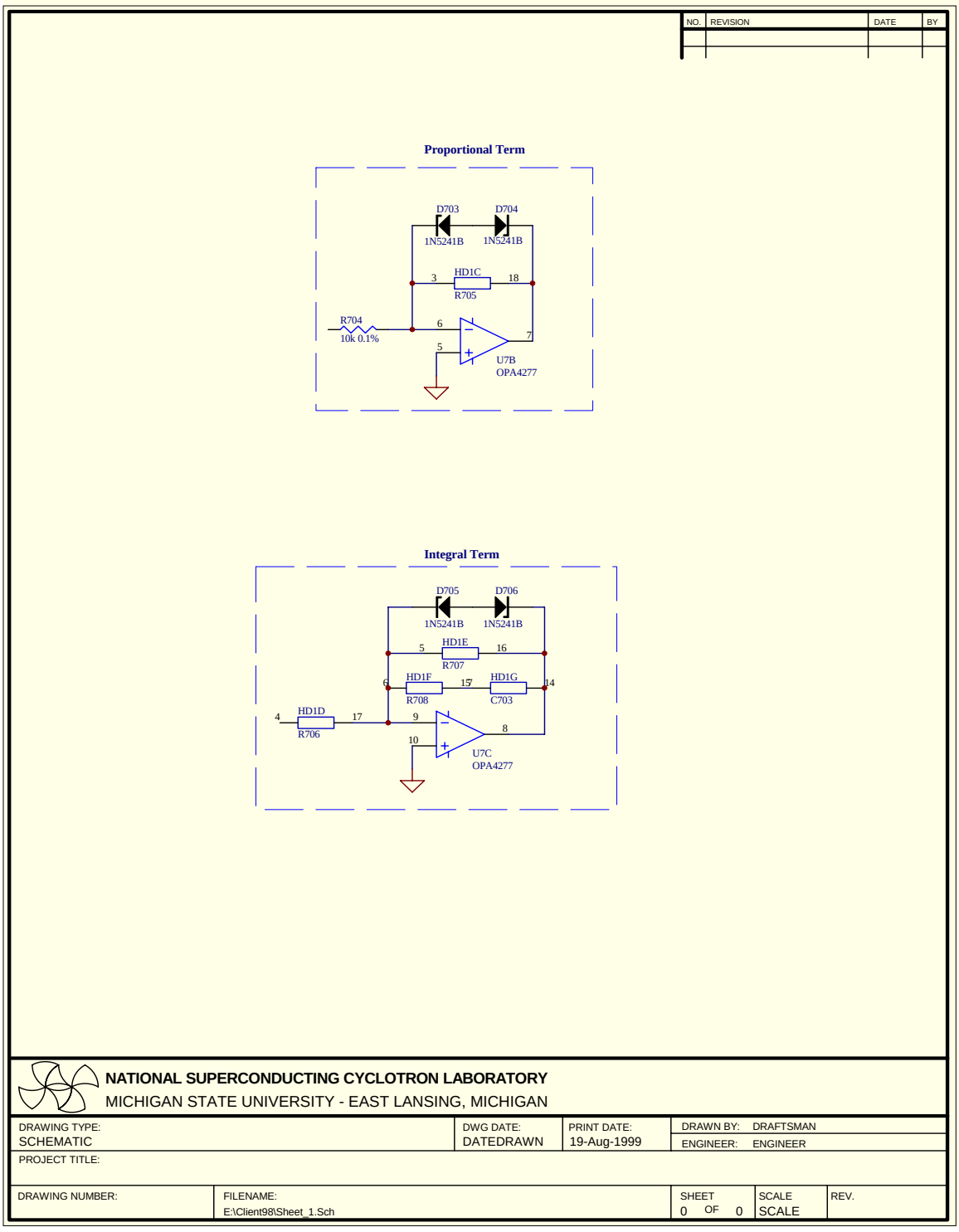

The proportional gain is derived from a simple inverting op-amp whose gain is given by

$$\boxed{K_P = \frac{R705}{R704}}$$

The lag-network is realized by an inverting op-amp with two parallel feedback paths. The one feedback path is a simple resistor, R707, and the other feedback path is a series RC combination, R708 and C703. The transfer function for the shown circuit is given as

$$\boxed{Lag(s) = K_I \cdot \frac{(s+z)}{(s+p)}}$$

with $\boxed{K_I = \frac{(R707 \,//\, R708)}{R706}}$

(where // means the parallel combination)

$$\boxed{z = \frac{1}{R708 \cdot C703}} \text{ in radians}$$

and

$$\boxed{p = \frac{1}{(R707 + R708) \cdot C703}} \text{ in radians}$$

Given the desired K_I , z, and p the best way to find component values is to proceed as follows:

1.) Choose C703

2.) Calculate the required R708 as $\boxed{R708 = \frac{1}{z \cdot C703}}$ (Ohms).

3.) Calculate the required R707 as $\boxed{R707 = \frac{1}{p \cdot C703} - R708}$ (Ohms).

4.) Calculate the required R706 as $\boxed{R706 = \frac{R707 \cdot p}{K_I \cdot z}}$ (Ohms)

Based upon the final designs for both the K500 and the K1200, the component values that will realize these designs are tabulated below. Note that the designed components are the same for both the K500 and the K1200 based upon the choice of K_p and K_I for both designs. These values may change once the actual system is calibrated and tuned.

Calculated K500 Controller Components

K_P Gain	R705 (kΩ)	K_I	z (Hz)	p (Hz)	C703 (pF)	R708 (kΩ)	R707 (kΩ)	R706 (kΩ)
0.4	4	0.5	10000	1	6800	2.34	23403.49	4.68

Calculated K1200 Controller Components

K_P Gain	R705 (kΩ)	K_I	z (Hz)	p (Hz)	C703 (pF)	R708 (kΩ)	R707 (kΩ)	R706 (kΩ)
0.4	4	0.5	10000	1	6800	2.34	23403.49	4.68

The actual component values used (due to available values), are tabulated below.

Actual K500 Controller Components

R705 (kΩ)	K_P Gain	R706 (kΩ)	R707 (kΩ)	R708 (kΩ)	C703 (pF)	p (Hz)	z (Hz)	K_I
4.02	0.40	4.64	22000	2.32	6800	1.06	10088.72	0.50

Actual K1200 Controller Components

R705 (kΩ)	K_P Gain	R706 (kΩ)	R707 (kΩ)	R708 (kΩ)	C703 (pF)	p (Hz)	z (Hz)	K_I
4.02	0.40	4.64	22000	2.32	6800	1.06	10088.72	0.50

The Motherboard Component Header

Due to the different compensation designs for the K500 and the K1200 a component header was designed onto the motherboard as a quick method of changing the tuning parameters. This component header also contains the feedback scaling for the peak-detector output that was discussed at the beginning of this note.

Furthermore, the component header also handles an additional gain for scaling the front-panel display meter. The full-scale display should be $100KV_{pk}$ for the K500 and $200KV_{pk}$ for the K1200. The internal control system full-scale level is 10V, while the meter displays 199.99 for a 2V signal. Thus, for the K500, 10V is scaled down to 1V and for the K1200, 10V is scaled down to 2V. The component that handles this is component R803.

A block diagram of the component header and its associated components is shown below:

Components Header (HD1)			
	Component		**Description**
Pin 1	R803	**Pin 20**	Meter Display Scaling Resistor
Pin 2	R608	**Pin 19**	Feed Forward Gain Resistor
Pin 3	R705	**Pin 18**	Proportional Gain Resistor
Pin 4	R706	**Pin 17**	Integral Op-Amp Input Resistor
Pin 5	R707	**Pin 16**	Integral LF Gain Resistor
Pin 6	R708	**Pin 15**	Integral HF Gain Resistor
Pin 7	C703	**Pin 14**	Integral Capacitor
Pin 8	R112	**Pin 13**	Peak-Detector Scaling Resistor1
Pin 9	R113	**Pin 12**	Peak-Detector Scaling Resistor2
Pin 10		**Pin 11**	

The proper component values for both the K500 and the K1200 are given below:

Component Header (HD1) Values

Component	K500	K1200
R803	1 KΩ	2 KΩ
R608	open	open
R705	4.02 KΩ	4.02 KΩ
R706	4.64 KΩ	4.64 KΩ
R707	22 MΩ	22 MΩ
R708	2.32 KΩ	2.32 KΩ
C703	6800 pF	6800 pF
R112	2.52 KΩ	2.67 KΩ
R113	15 KΩ	17.4 KΩ

Conclusion

The design of the dee-voltage regulation systems for both the K500 and the K1200 was based upon both theoretical formulations and experimental investigations. The final designs were determined by matching the theoretical model to experimental results that were performed on the K1200 system. Although there is much confidence in the designs, they will still need to be confirmed on the actual systems. The tables of overshoot and disturbance rejection versus proportional and integral gain can be used to fine tune the actual systems.

The closed-loop calibration procedure that is to be followed is:

1.) Determine the actual attenuator values versus frequency by performing a dee-voltage x-ray calibration procedure.
2.) Tune the system to the highest RF operating frequency, 26.5MHz and use the attenuator value determined from step 1.
3.) With the DVR in open-loop, condition the system to hold the maximum desired dee-voltage. Adjust the full-scale DVR RF output on the RF Amplitude-Controller board if needed.
4.) Once the system is at the maximum desired dee-voltage at 26.5MHz and has had ample time to come to thermal equilibrium, simultaneously adjust both the front panel control knob and the full-scale DVR RF output on the RF Amplitude-Controller board such that 10.0V from the control knob corresponds to the maximum dee-voltage. Thus, the open-loop gain is normalized to unity for the maximum dee-voltage at 26.5MHz.
5.) Take a measurement of the open-loop gain as a reference for the open-loop gain at other RF frequencies. This is done by measuring the DVR RF output level at a specific dee-voltage. The open-loop gain value is defined as (dee-voltage/DVR output).
6.) Test the system in closed-loop at 26.5MHz. Use the overshoot and disturbance rejection ratio tables to tune the closed-loop controller components if needed. The overshoot should be adjusted such that the system has no problems turning-on and such that the disturbance rejection is optimal. The disturbance rejection can be measured by taking an FFT of both the open-loop and closed-loop noise on the feedback signal. This completes the calibration at 26.5MHz.
7.) Next, tune the system for the lowest RF operating frequency (9.5MHz for the K1200, 11MHz for the K500) using the attenuator value determined in step 1. Measure the open-loop gain for the maximum dee-voltage at 9.5MHz. (see maximum dee-voltage vs. frequency charts from this note). Confirm that this open-loop gain value is less than 1.5 times the open-loop gain at 26.5MHz. If it is not, the tuning of the closed-loop controller components may have to be repeated.
8.) Test the system in closed-loop at this lowest RF frequency. Make sure the system turns on properly. Take a measurement of the disturbance rejection ratio as in step 5. If any tuning of the controller components needs to be done, use the overshoot and disturbance rejection tables from this note. Also repeat steps 4-7 until the system has been fine-tuned at both RF frequency extremes.

Appendix A

Amplitude Modulation in a Resonant Cavity

At resonance, a resonant electromagnetic cavity is usually represented as a parallel RLC circuit, whose resistance value, R_s , is determined from its loses at resonance and whose reactive values are determined from the energy stored at resonance. The ratio between the energy stored in the reactive components and the loses in the resistive component at resonance gives a measurement of the resonator's quality factor, Q. It is intuitive that this Q-factor will influence the response of a resonant structure to amplitude modulations. To see this link a bit more clearly let us consider the following:

Amplitude modulation of a carrier frequency generates a frequency spectrum equivalent to the spectrum of the modulating signal centered about the carrier frequency. Thus, let us consider the scenario that a resonant cavity is being driven at it's resonance frequency, but that the amplitude of the driving signal is being modulated. We then wish to detect the amplitude fluctuations with a probe on the resonant cavity. As the frequency of the amplitude modulating signal increases the sidebands of the resultant modulated spectrum will be pushed outside of the resonator's bandwidth and will thus suffer a dampening effect due to the resonator's frequency selectivity. For instance, if the resultant frequency spectrum of the modulated carrier far exceeded the bandwidth of the resonator, the applied signal wouldn't even make it into the resonator.

Now if we wished to mathematically characterize the resonator's response to amplitude modulations, we could make a first approximation by assuming the response would have a low-pass filter response to amplitude modulating signals. Previously this low-pass filter was approximated with a single pole, but a more thorough mathematical analysis of the situation proves that this single pole approximation is only valid for very low Q-factors.

The complete mathematical analysis is initiated by assuming that the resonant cavity can be modeled as a parallel RLC circuit within the quality factor bandwidth. We begin by determining the transfer function relating the output voltage to the driving current of a parallel RLC circuit. The transfer function turns out to be the expression for the impedance of the circuit as a function of frequency, given as

$$Z(f) = \frac{V(f)}{I(f)} = \frac{j\dfrac{2\pi f}{C}}{\dfrac{1}{LC} + j\dfrac{2\pi f}{RC} - (2\pi f)^2} \quad . \qquad (1)$$

Now, when we apply amplitude modulation (or narrowband phase modulation PM) to the RF drive signal, we are applying a signal with a certain frequency spectrum. This frequency spectrum is then applied to the resonator which acts as a filter. When we then detect the voltage (or phase) we are demodulating by shifting the filtered spectrum down to a baseband for which DC corresponds to the non-modulated carrier RF frequency. This demodulation process is mathematically equivalent to multiplying the filtered signal by a sinusoid whose frequency is equal to the resonant frequency of the parallel RLC circuit.

In the frequency domain, the demodulation process is described mathematically with the use of Fourier transforms. The modulation theorem is given as

$$s(t)\cdot\cos(2\pi f_R t) \Leftrightarrow \frac{1}{2}S(f - f_R) + \frac{1}{2}S(f + f_R) \quad . \qquad (2)$$

To find the response of the system to amplitude modulations, we would apply a delta function modulating signal input. Thus, $s(t)$ becomes the delta function $\delta(t)$. And since,

$$\delta(t)\cdot\cos(2\pi f_R t) = \delta(t) \Leftrightarrow 1 \ , \qquad (3)$$

Thus, the final system is expressed mathematically as

$$Z(f)\otimes\Im\{\cos(2\pi f_R t)\} = \frac{1}{2}Z(f - f_R) + \frac{1}{2}Z(f + f_R) \ , \qquad (4)$$

where use of the modulation theorem was made. Using the expression for $Z(f)$ as given in (1), equation (4) can be expanded into

$$\frac{1}{2}Z(f-f_R)+\frac{1}{2}Z(f+f_R)=$$

$$\frac{1}{2}\cdot\frac{j\frac{2\pi f}{C}-j\frac{2\pi f_R}{C}}{\frac{1}{LC}+\frac{1}{RC}j2\pi f-\frac{1}{RC}j2\pi f_R-(2\pi f)^2+2\pi f\cdot 4\pi f_R-(2\pi f_R)^2}+$$

$$\frac{1}{2}\cdot\frac{j\frac{2\pi f}{C}+j\frac{2\pi f_R}{C}}{\frac{1}{LC}+\frac{1}{RC}j2\pi f+\frac{1}{RC}j2\pi f_R-(2\pi f)^2-2\pi f\cdot 4\pi f_R-(2\pi f_R)^2}$$

The terms involving f were purposely kept separate from those terms involving f_R. The reason is that in order to convert to the LaPlace transform, which is extensively used for control system theory, $j2\pi f$ is replaced by the variable s. The resulting LaPlace transform expression for the cyclotron's response to amplitude modulations is

$$Z(s)=\frac{s^3LCR+s^2L+s\,(R+4\pi^2 f_R{}^2LCR)+4\pi^2 f_R{}^2L}{s^4(LCR)^2+s^3 2L^2CR+s^2[L^2+2LCR^2+8\cdot(\pi f_R LCR)^2]+s\;[2RL+8CR(\pi f_R L)^2]+\ldots}$$
$$\ldots[R^2+(4\pi^2 f_R{}^2LCR)^2-8LC(\pi f_R R)^2+(2\pi f_R L)^2]$$

For typical values for R, L, and C, the above transfer function results in a system which has one real zero, one pair of complex conjugate zeros, and two pairs of complex conjugate poles. The overall system exhibits a combinatory behavior of both a low-pass filter, LPF, and a band-pass filter, BPF. The real zero and the pair of complex conjugate poles closest to this zero compose the LPF, while the pair of complex conjugate zeros and the remaining pair of complex conjugate poles compose the BPF. The BPF has a center frequency equal to twice the cavity's resonant frequency, f_R. Our voltage peak detectors (and digital phase detectors) end up blocking this portion of the frequency spectrum since they are inherently low-pass in nature. This is true since they don't really incorporate mixing in the voltage (phase) detecting process. However, true mixing detectors will generate a frequency spectrum that occupies the region within the BPF region. But in those cases, since it is only the low-frequency amplitude (phase) oscillations which are physically occuring, a LPF on the detector's output blocks out the added harmonic components which are generated in the mixing process. Thus, we are only concerned with the LPF realized by the real zero and the complex conjugate pole pair.

Although a thorough mathematical formulation is not given for the following discussion, it is clearly observed with practical component values:

> A resonator's response to small phase modulations is approximately equivalent to a resonator's response to amplitude modulations. Using a parallel RLC equivalent circuit model for an electromagnetic resonator, the amplitude modulation response was determined mathematically, using Fourier transforms, to be a LPF-like function, but it does not consist of a single pole. Instead, it consists of one real zero and two complex conjugate poles. In the limit as Q approaches infinity, the two complex conjugate poles close in on the real zero, thereby resulting in a single-pole LPF after a pole/zero cancellation. However, this single-pole also approaches zero in the limit as Q approaches infinity and thus, the resonator becomes practically incapable of supporting any sort of amplitude modulations. As the Q-factor is lowered, the zero/complex-conjugate-pole pair moves increasingly to the left in the s-plane while simultaneously becoming more separated.

In conclusion, the cyclotron's response to amplitude modulations and narrowband phase modulations will be modeled with the appropriate single zero and complex conjugate pole pair which can be determined from finding the roots of the numerator and denominator polynomials of equation (6). These roots can be found using any mathematical tools. The lowest valued complex conjugate poles will be the ones corresponding to the low-pass filter and the highest valued pair will be those corresponding to the band-pass filter.

In the specific case of the K1200 and CCP K500 cyclotrons, the shunt resistance value, R_S, can be determined from power loss measurements on the resonant structure. Such measurements were done on the K1200 in John Vincent's dissertation.. As for measurements of the stored energy, which determines the reactive element values, no actual data exists for either cyclotron. Simulated values exist for both the K1200 and the CCP K500 and can be used for initial models.